Long-Range Interacting Systems

Thierry Dauxois
École Normale Supérieure de Lyon, CNRS, France

Stefano Ruffo
Università di Firenze, INFN, Firenze, Italy

Leticia Cugliandolo
Université Pierre et Marie Curie - Paris VI, France

OXFORD
UNIVERSITY PRESS

Contents

Part I

Statistical Dynamics

Part II

Hydrodynamics

Part III

Mathematical Aspects

Part IV

Gravitational Interaction

Part V

Coulomb and Wave-Particle interaction

16
Plasma Collisional Transport

Daniel H.E. Dubin

University of California at San Diego, Physics Department 0319, 9500 Gilman Drive, La Jolla CA 92093 USA

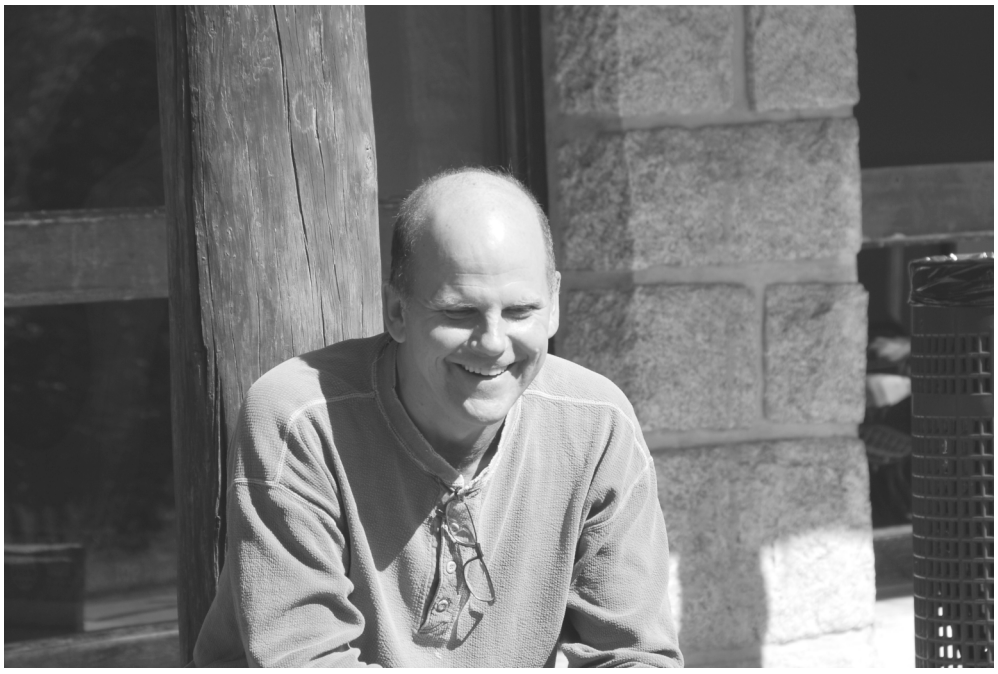

16.1 Estimates

The question addressed in the following lectures dates from the earliest days of plasma physics research: how do collisions in a plasma affect the transport (i.e., redistribution) of energy, momentum, and particles? Surprisingly, several aspects of this venerable problem remain incompletely understood. As befits lectures at a school on long-range interactions, many of these thorny issues relate to the long-range nature of the Coulomb interaction.

We will first review some basic concepts relating to collisions in plasmas. Consider a particle of mass m with velocity $\mathbf{v} = (v_x, v_y, v_z)$. The probability density associated with the velocity is, in thermal equilibrium, given by a Maxwellian distribution,

$$f_{\max}(\mathbf{v}) = \frac{e^{-mv^2/2T}}{(\sqrt{2\pi T/m})^3}, \tag{16.1}$$

where T is the temperature. The thermal speed $\bar{v}$ of a collection of particles with temperature T is the RMS velocity associated with this distribution,

$$\begin{aligned}\bar{v}^2 &= \int d^3v\, v_x^2 f_{\max}(v) = \int d^3v\, v_y^2 f_{\max} = \int d^3v\, v_z^2 f_{\max} \\ &= T/m.\end{aligned} \tag{16.2}$$

Exercise 16.1 For two particles taken from distribution (16.1), show that the distribution of their relative velocities, $\mathbf{v}_r = \mathbf{v}_1 - \mathbf{v}_2$, is also Maxwellian but at twice the temperature:

$$f_{\rm rel}(v_r) = \frac{e^{-mv_r^2/4T}}{(\sqrt{4\pi T/m})^3} \tag{16.3}$$

To estimate the rate of collisions ν between particles, assuming they all have charge e, we rather arbitrarily define this rate as the mean rate at which the relative velocity for two colliding particles scatters by 90° or more. Two particles separated by impact parameter ρ (see Fig. 16.1) and with initial relative velocity $\mathbf{v}_r = \mathbf{v}_1 - \mathbf{v}_2$ require, for scattering 90° or more, that

$$\rho \lesssim \frac{e^2}{mv_r^2}. \tag{16.4}$$

The rate ν at which such collisions occur is

$$\nu = \int d^3v_r\, n f_{\rm rel}(v_r) v_r \times \int_0^{e^2/mv_r^2} 2\pi\rho d\rho \tag{16.5}$$

where n is the particle density. The first integral in this expression gives the flux of particles impacting on a given charge, and the second integral over impact parameters

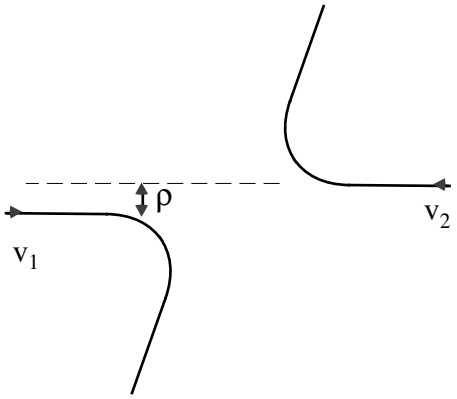

Fig. 16.1 Collision between two particles in an unmagnetized plasma.

estimates the cross-section for 90° scattering. Performing the ρ integral and using eqn (16.3) yields

$$\nu = \frac{\sqrt{\pi}}{2} n \bar{v} b^2 \int_{v_{\min}}^{\infty} \frac{dv_r \, e^{-v_r^2/4\bar{v}^2}}{v_r}, \tag{16.6}$$

where $b \equiv e^2/T$ is the distance of closest approach, and we have introduced a lower cutoff $v_{\min}$ to the relative velocity integral since otherwise the integral diverges logarithmically. Such divergences are a common problem in plasma kinetic theory, and extra physical effects must be added to the model to determine the cutoffs. In this case, we note that $v_r \to 0$ is equivalent to the maximum impact parameter approaching ∞ [see Eqn. (16.4)], so $v_{\min}$ is set by the maximum reasonable ρ. This is usually taken to be the Debye length λ_D, defined as

$$\lambda_D \equiv \sqrt{T/4\pi e^2 n}, \tag{16.7}$$

which implies that

$$v_{\min} = \sqrt{\frac{e^2}{m\lambda_D}}. \tag{16.8}$$

The Debye length is the length over which potentials are shielded out in a plasma. If a stationary test charge Q is placed in a plasma consisting of two species with charges $\pm e$ at densities $n_+ = n_- = n$, in thermal equilibrium the density is perturbed by the presence of Q according to Boltzmann distributions

$$n_{\substack{+ \\ (-)}} = n \, e^{\mp e\phi/T}, \tag{16.9}$$

where ϕ is the potential, which satisfies Poisson's equation

$$\nabla^2 \phi = -4\pi Q \delta(\mathbf{r}) - 4\pi e n_+ + 4\pi e n_-. \tag{16.10}$$

Substituting for n_+ and n_-, linearizing in ϕ (assuming $e\phi/T \ll 1$) and solving yields

$$\phi(r) = Q\,\frac{e^{-\sqrt{2}r/\lambda_D}}{r}. \tag{16.11}$$

The factor of $\sqrt{2}$ arises because two species do the shielding: like charges are repelled from Q and opposite charges are attracted, and each shielding effect is additive. Returning to our expression for the collision rate we note that $v_{\rm min} \ll \bar{v}$ for typical plasmas for which $\lambda_D/b \gg 1$, in which case, to "logarithmic accuracy," the velocity integral in eqn (16.6) can be approximated by

$$\int_{v_{\rm min}}^{\bar{v}} \frac{dv_r}{v_r} \cong \ln\left(\frac{\bar{v}}{v_{\rm min}}\right) = \frac{1}{2}\ln\left(\frac{\lambda_D}{b}\right), \tag{16.12}$$

where in the second form we substituted for $v_{\rm min}$ from eqn (16.8). This approximation to the actual integral in eqn (16.6) neglects an additive constant of order unity, which is reasonable provided that $\ln(\lambda_D/b) \gg 1$. Typical values of $\ln(\lambda_D/b)$ are of order 10 in the experiments we will consider later. In other words, a change in our estimate of $v_{\rm min}$ by a factor of 2 makes only a small change in ν. That is why only an estimate of $v_{\rm min}$ is needed. Thus, the collision rate in a plasma scales as (Spitzer 1956; Montgomery and Tidman 1964)

$$\nu \sim n\bar{v}\,b^2 \ln\left(\frac{\lambda_D}{b}\right), \tag{16.13}$$

$$\equiv \nu_0 \ln\left(\frac{\lambda_D}{b}\right). \tag{16.14}$$

As density increases ν increases since collisions become more likely; and as temperature increases ν decreases because higher velocity particles are harder to deflect. The rate $\nu_0 \equiv n\bar{v}b^2$ will appear often in the following analyses.

Exercise 16.2 Estimate ν for a virialized globular cluster of 10^6 solar mass stars, with mean density 1 star/cubic light year. Note that Debye shielding does not occur in self gravitating systems, so λ_D must be replaced by the system radius.

16.1.1 Transport in Unmagnetized Plasmas

The mean free path ℓ of a particle is the mean distance the particle travels between collisions, given by

$$\ell \simeq \bar{v}/\nu. \tag{16.15}$$

After each collision time ν^{-1}, the particle's velocity is randomized, so that its path resembles a "random walk" with step size of order ℓ. This leads to diffusion of a distribution of such particles: the mean square change in position increases linearly with time t, as

$$\langle[\mathbf{r}(t) - \mathbf{r}(0)]^2\rangle = 2Dt/3. \tag{16.16}$$

Here, the average $\langle\ \rangle$ is over the distribution of initial conditions and D is the particle diffusion coefficient, which may be estimated as

$$D \cong \nu \ell^2 \sim \frac{\bar{v}^2}{\nu}. \tag{16.17}$$

Equation (16.17) also holds in gases with short-range interactions; the long-range nature of the Coulomb interaction does not affect this estimate. Smaller collision frequency implies larger diffusion, due to the increase in the mean free path.

The particle density $n(x,t)$ for a diffusive process follows the diffusion equation

$$\frac{\partial n}{\partial t} = \frac{\partial}{\partial x} D \frac{\partial n}{\partial x}. \tag{16.18}$$

Similar equations govern the transport of energy and momentum in a plasma. A plasma with a nonuniform temperature $T(x,t)$ evolves through collisions according to the heat equation,

$$C \frac{\partial T}{\partial t} = \frac{\partial}{\partial x} \kappa \frac{\partial T}{\partial x} \tag{16.19}$$

where C is the specific heat and κ is the thermal conductivity. The ratio $\chi = \kappa/C$ has units of a diffusion coefficient and is termed the thermal diffusivity. Similarly momentum transport in a system for which the fluid velocity is sheared, $\mathbf{V} = V_y(x,t)\hat{y}$, is also governed by a diffusion equation:

$$mn \frac{\partial V_y}{\partial t} = \frac{\partial}{\partial x} \eta \frac{\partial V_y}{\partial x} \tag{16.20}$$

where η is the shear viscosity (we do not consider flows for which bulk viscosity is important). The ratio $\lambda = \eta/mn$ also has dimensions of a diffusion coefficient and is called the kinematic viscosity.

In an unmagnetized plasma

$$\chi \sim \lambda \sim D, \tag{16.21}$$

since particles carry their energy and momentum with them as they diffuse (Spitzer 1956; Simon 1955; Spitzer and Harm 1952).

16.1.2 Magnetized Plasma: Classical Theory of Collisional Transport

When a uniform magnetic field $\mathbf{B} = B\hat{z}$ is applied, collisional transport is reduced in the directions transverse to the field. This is because an isolated charge no longer travels in a straight line trajectory, but rather executes circular cyclotron motion with radius $r_c = \frac{v_\perp}{\Omega_c}$, where $v_\perp = \sqrt{v_x^2 + v_y^2}$ is the perpendicular particle speed and $\Omega_c = eB/mc$ is the cyclotron frequency, which is the frequency (in radians/sec) of the circular motion. For an isolated particle the center of the circular orbit, termed the "guiding center" position, is fixed (except for the uniform motion along $\mathbf{B}$). However, when two particles collide, the guiding centers of the two particles step across the magnetic field.

In classical transport theory this cross-field step happens because of the velocity scattering that we described previously in an unmagnetized plasma. In the collision, the perpendicular velocity $\mathbf{v}_\perp$ for each particle changes leading to a change $\Delta\mathbf{r}$ in the guiding center position; see Fig. 16.2. The mean size of such steps is of order

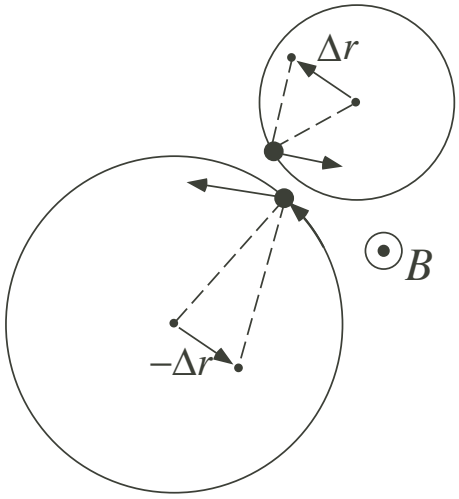

Fig. 16.2 Typical collision between two particles in a magnetized plasma.

$$\bar{r}_c = \bar{v}/\Omega_c, \tag{16.22}$$

the mean cyclotron radius. The rate of these steps is the collision rate ν, so we can estimate the diffusion coefficient as

$$D = \nu \bar{r}_c^2. \tag{16.23}$$

Comparing to eqn (16.17), we see that the mean free path has been replaced by the cyclotron radius because the magnetic field limits the cross-field motion to a distance of order $\bar{r}_c$. Again, thermal diffusivity and kinematic viscosity are of order D. These coefficients were worked out rigorously in the early days of plasma physics (Spitzer 1956; Longmire and Rosenbluth 1956; Simon 1956; Rosenbluth and Kaufmann 1958; Braginskii 1958; Braginskii 1965), and are given in Table 16.1.[1] Interestingly, to my knowledge none of these coefficients have ever been measured experimentally to better than order of magnitude accuracy, mainly because of the difficulty of producing a quiescent magnetized plasma where collisional transport is not swamped by competing effects such as instabilities or turbulence.

16.1.3 Long-Range Collisions

The classical theory has been used for decades to evaluate transport due to collisions in a magnetized plasma. However, the validity of the theory is limited by the assumption that transport is due primarily to collisions that scatter the perpendicular velocity vector. In fact, collisions with large impact parameters ("long-range" collisions) that do not lead to appreciable velocity scattering can dominate the collisional transport.

[1]Not all authors agree on the values of the numerical coefficients for χ and λ. The coefficients quoted in Table 16.1 are those given in Braginskii (1965) for ion-ion collisions.

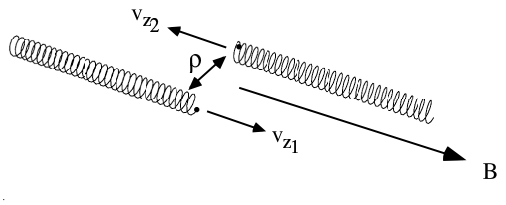

Fig. 16.3 Typical collision with impact parameter $\rho \sim \lambda_D$ between two particles in a magnetized plasma where $\bar{r}_c \ll \lambda_D$.

For example, consider the situation where the magnetic field is sufficiently strong so that $\lambda_D > \bar{r}_c$. The velocity-scattering collisions pictured in Fig. 16.2 occur only for guiding centers separated across $\mathbf{B}$ by a distance of order $\bar{r}_c$; but many more collisions occur with larger impact parameters ρ of order λ_D. These collisions do not look like those in Fig. 16.2; such a collision is shown in Fig. 16.3.

No appreciable perpendicular velocity scattering occurs in these collisions, but momentum and energy are still transported across the magnetic field. For instance, consider energy transport. Through such long-range collisions, a particle on one magnetic field line can transfer parallel energy to a particle on a field separated by a Debye length (by exchange of parallel velocities). The distance over which energy is transfered is now λ_D, with exchanges occurring at rate ν, so the thermal diffusivity is

$$\chi \sim \nu \lambda_D^2. \tag{16.24}$$

This is much larger than that given by the classical theory (Table 16.1) when $\lambda_D > \bar{r}_c$ (Psimopolis and Li 1992; Dubin and O'Neil 1997). A similar argument for momentum transport yields kinematic viscosity

$$\lambda \sim \nu \lambda_D^2 \tag{16.25}$$

as well (O'Neil 1985).

Furthermore, the exchange of energy and momentum is not limited to interactions between particles separated by only λ_D. Particles can transfer energy by emitting and absorbing weakly-damped waves that travel large distances across the plasma (Rosenbluth and Liu 1976; Dubin and O'Neil 1997). While the impact parameter for such "collisions" is limited only by the plasma size, the effective rate of collisions is smaller than ν because the fluctuation energy in lightly-damped plasma waves is a small fraction of the total fluctuation energy in the plasma. Even so, we will see that detailed calculations predict lightly damped waves can dominate the energy and momentum transport in plasmas that are sufficiently large.

Particle diffusion also occurs due to the long-range collisions shown in Fig. 16.3. The origin of the diffusion is the $\mathbf{E} \times \mathbf{B}$ drift that occurs as charges encounter one another (Lifshitz and Pitaevskii 1981). To understand $\mathbf{E} \times \mathbf{B}$ drifts, consider the dynamics of a particle in a uniform magnetic field $B\hat{z}$ *and* a uniform electric field $E\hat{x}$. The particle's motion is given by

$$m\frac{d\mathbf{v}}{dt} = e\left(\mathbf{E} + \frac{\mathbf{v}\times\mathbf{B}}{c}\right). \tag{16.26}$$

The solution to this linear ODE for $\mathbf{v}(t)$ is a sum of a particular and homogeneous solution. The homogeneous solution is simply the circular cyclotron motion described previously. The particular solution (for the case where $\mathbf{E}\perp\mathbf{B}$) is

$$\mathbf{v}_{E\times B} = \frac{\mathbf{E}\times\mathbf{B}}{B^2}c = -\frac{E}{B}c\hat{y}. \tag{16.27}$$

This velocity, the $\mathbf{E}\times\mathbf{B}$ drift, is superimposed on the cyclotron motion.

Now consider the collision between two particles, shown in Fig. 16.3. Assuming that $\Omega_c \gg v_r/\lambda_D$ and $\lambda_D \gg r_c$, the electric field between the charges varies slowly compared to the cyclotron motion and can be taken to be nearly uniform in space and time. This immediately leads to an $\mathbf{E}\times\mathbf{B}$ drift velocity due to the perpendicular component of $\mathbf{E}$, given by eqn (16.27), which for an electric field of order e/λ_D^2 yields

$$v_{E\times B} \sim \frac{e}{\lambda_D^2 B}c. \tag{16.28}$$

This drift acts for a time $t_d \sim \lambda_D/v_r \sim \lambda_D/\bar{v}$ as particles pass one another, implying a cross-magnetic-field step $\Delta r = v_{\mathbf{E}\times\mathbf{B}}t_d$, or

$$\Delta r \sim \frac{e}{\lambda_D B}\frac{c}{\bar{v}}. \tag{16.29}$$

The rate of these collisions is roughly $n\bar{v}\lambda_D^2$, so the particle diffusion coefficient D is

$$\begin{aligned} D &\sim n\bar{v}\lambda_D^2\,\Delta r^2 \\ &= \nu_0\bar{r}_c^2, \end{aligned} \tag{16.30}$$

neglecting constants of order unity and logarithmic factors. Thus $\mathbf{E}\times\mathbf{B}$ drift diffusion due to long-range collisions has roughly the same scaling as the diffusion due to the velocity scattering described by the classical theory (Lifshitz and Pitaevskii 1981; Anderegg *et al.* 1997; Dubin 1997). In lecture 2 we will see that in one set of experiments the $\mathbf{E}\times\mathbf{B}$ diffusion is about 10 times the classical theory.

It should be noted that velocity-scattering collisions still occur when $\lambda_D > \bar{r}_c$, due to collisions with impact parameter $\rho \lesssim \bar{r}_c$. The classical transport coefficients describe these collisions, except that the maximum impact parameter appearing in the Coulomb logarithm is no longer λ_D, but rather $\bar{r}_c$ (Montgomery *et al.* 1974). When $\lambda_D > \bar{r}_c$ the total transport is a sum of classical transport due to collisions with impact parameters ρ less than $\bar{r}_c$, and long range transport due to collisions with $\rho > \bar{r}_c$.

16.2 Kinetic Theory of E x B Drift Diffusion, and Experiments

16.2.1 Integration Along Unperturbed Orbits

In this lecture we will rigorously calculate the diffusion due to $\mathbf{E}\times\mathbf{B}$ drifts that we estimated in the previous lecture, and we will compare the result to experimental

Table 16.1 Classical Theory of Collisional Transport

D	χ	λ
$\frac{4}{3}\sqrt{\pi}\nu_0\bar{r}_c^2\ln(\frac{\rho_{\max}}{b})$	$\frac{16}{9}\sqrt{\pi}\nu_0\bar{r}_c^2\ln(\frac{\rho_{\max}}{b})$	$\frac{2}{5}\sqrt{\pi}\nu_0\bar{r}_c^2\ln(\frac{\rho_{\max}}{b})$

$\nu_0 = n\bar{v}b^2, \quad \rho_{\max} = \begin{cases} \lambda_D\ , \lambda_D<\bar{r}_c \\ \bar{r}_c\ , \lambda_D>\bar{r}_c \end{cases}$

measurements (Anderegg *et al.* 1997). As before, we assume an infinite uniform plasma in the regime $\lambda_D > \bar{r}_c$, and concentrate on the motion of the guiding centers only since cyclotron motion is not important in this process.

We consider the interaction of two like particles, labeled 1 and 2, following the motion of the guiding centers. Equations of motion for the guiding center of particle 1, at position $\mathbf{r}_1 = (x_1, y_1, z_1)$ with axial velocity v_{z_1}, are

$$\frac{dx_1}{dt} = -\frac{c}{eB}\frac{\partial\phi_{12}}{\partial y_1}, \quad \frac{dy_1}{dt} = \frac{c}{B}\frac{\partial\phi_{12}}{\partial x_1}, \quad \frac{dz_1}{dt} = v_{z_1}, \quad \frac{dv_{z_1}}{dt} = -\frac{1}{m}\frac{\partial\phi_{12}}{\partial z_1} \tag{16.31}$$

where $\phi_{12} = e^2/|\mathbf{r}_1 - \mathbf{r}_2|$ is the Coulomb potential energy. For particle 2 the equations of motion are obtained by interchanging labels 1 and 2 in eqns 16.31).

As the particles pass one another, they step across the magnetic field. The step in the x direction for particle 1, δx_1, is given by integrating dx_1/dt:

$$\delta x_1 = \frac{ce}{B}\int_{-\infty}^{\infty} dt \frac{y_1 - y_2}{[(x_1 - x_2)^2 + (y_1 - y_2)^2 + (z_1 - z_2)^2]^{3/2}}. \tag{16.32}$$

In order to evaluate this integral, we assume that the interaction between the particles only weakly perturbs the particle orbits, so we use the unperturbed orbits in the integrand, taking $z_r \equiv z_1 - z_2 = v_r t$, $x_1 - x_2 = \text{const.}$, $y_1 - y_2 = \text{const.}$ This well-known approximation method is called the method of integration along unperturbed orbits (IUO). Then eqn (16.32) yields

$$\delta x_1 = \frac{2ce}{B|v_r|\rho^2}(y_1 - y_2), \tag{16.33}$$

where $\rho = \sqrt{(x_1 - x_2)^2 + (y_1 - y_2)^2}$ is the impact parameter. This result has the same scaling as the previous estimate, eqn (16.29).

Diffusion of particle 1 can now be determined as a series of uncorrelated steps δx_1 due to collisions with an incident flux of particles 2 streaming past 1 along the magnetic field:

$$D = \frac{1}{2}\frac{\langle\Delta x^2\rangle}{\Delta t} = \frac{1}{2}\int_{-\infty}^{\infty} dv_r n f_{\text{rel}}(v_r)\int_0^{\infty}\rho\, d\rho\int_0^{2\pi} d\theta|v_r|(\delta x_1)^2. \tag{16.34}$$

Substituting for $(\delta x_1)^2$ from eqn (16.33) and for the distribution of relative z-velocities $f_{\text{rel}}(v_r) = e^{-mv_r^2/4T}/\sqrt{4\pi T/m}$, the integral over θ can be performed but the integrals over v_r and ρ must be cut off due to logarithmic divergences:

$$D = \frac{1}{2}\left(\frac{2ce}{B}\right)^2 \frac{n}{\sqrt{4\pi T/m}} 2\int_{\rho_{\min}}^{\rho_{\max}} \frac{d\rho}{\rho}\int_{v_{\min}}^{\infty} \frac{dv_r}{|v_r|} e^{-mv_r^2/4T}. \tag{16.35}$$

We deal with the logarithmically-divergent ρ integral by positing that Debye shielding acts to cut off the long-ranges, giving $\rho_{\max} = \lambda_D$, and that the $\mathbf{E}\times\mathbf{B}$ drift approximation breaks down at short ranges, giving $\rho_{\min} = \bar{r}_c$. For $\rho < \bar{r}_c$ the velocity scattering collisions described by the classical theory dominate. The classical diffusion arising from this range of impact parameters, given in Table 16.1, must be added to eqn (16.35).

The divergence in v_r is a bit more subtle. It comes about because when $v_r \to 0$, particles may interact for a long time and take a correspondingly large drift step–see eqn (16.33). Here we note that in reality particle velocities do not remain constant forever–collisions with surrounding particles cause v_r to diffuse, so even if it is initially zero it does not remain so. On average, particles with $v_r = 0$ initially will obey

$$\langle v_r^2 \rangle = 2D_v t \tag{16.36}$$

where D_v is the velocity diffusion coefficient due to collisions, $D_v \sim \nu\bar{v}^2$. Since, on average, $\sqrt{\langle v_r^2\rangle}$ increases like $\sqrt{D_v t}$, the rms relative z position $\sqrt{\langle z_r^2\rangle}$ will also increase, like $\sqrt{D_v}\,t^{3/2}$. The interaction between the particles is reduced by order unity once z_r has increased from 0 to ρ, which requires a time of order $(\rho/\sqrt{D_v})^{2/3}$. The mean relative speed over this time is $v_{\min} = \rho(\sqrt{D_v}/\rho)^{2/3} = (D_v\rho)^{1/3}$. Using this result in eqn (16.35) yields the following expression for the diffusion coefficient across the magnetic field due to $\mathbf{E}\times\mathbf{B}$ drifts in the regime $\lambda_D > \bar{r}_c$:

$$D_{\mathrm{IUO}} = 2\sqrt{\pi}\nu_0 r_c^2 \ \ln\left(\frac{\bar{v}}{|D_v\sqrt{\lambda_D r_c}|^{1/3}}\right)\ln\left(\frac{\lambda_D}{\bar{r}_c}\right) \tag{16.37}$$

where $\nu_0 \equiv n\bar{v}b^2$.

We label the diffusion coefficient as D_{IUO} because integration along unperturbed orbits was used in the derivation. We will find that this method needs to be modified, because integration along unperturbed orbits contains a subtle error.

Another effect, shear in the background plasma flow, can also set an effective minimum relative velocity. Particles separated by ρ would then have $v_{\min} \sim S\rho$ where $S = |\nabla\mathbf{V}|$ is the shear rate of the flow. Equation (16.37) assumes that S is sufficiently small that $v_{\min}$ is set by collisions, not shear.

16.2.2 Experiments

We will now compare this prediction to experimental measurements, performed in a pure ion plasma in our group at UCSD (Anderegg *et al.* 1997). The plasma is a collection of roughly 10^{10} Mg^+ ions confined in a Malmberg-Penning trap geometry, shown in Fig. 16.4. Cylindrical electrodes are biased so as to provide an axial potential well for the ions. Radial confinement is provided by an axial magnetic field. The plasma rotates about the axis of symmetry at frequency ω_r, providing a $\mathbf{v}\times\mathbf{B}$ force to balance the radial electric field E_r: radial force balance implies

$$\frac{e\omega_r r B}{c} = e\,E_r + m\omega_r^2 r \tag{16.38}$$

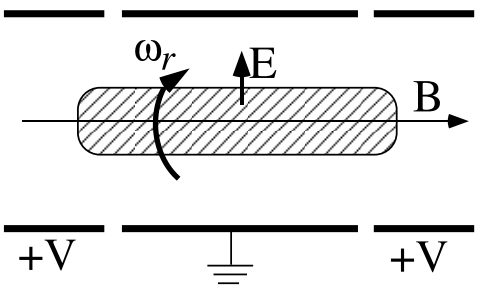

Fig. 16.4 Nonneutral plasma confined in a Malmberg-Penning trap.

and axial force balance implies $E_z = 0$ in the plasma. Solving eqn (16.38) for E_r and applying Poisson's equation $\nabla \cdot \mathbf{E} = 4\pi e n$, we obtain the following relation between rotation frequency and density:

$$n = \frac{m\omega_r}{2\pi e^2}(\Omega_c - \omega_r). \tag{16.39}$$

Pure ion plasmas can be confined in a quiescent near thermal-equilibrium state for arbitrarily long time periods (Dubin and O'Neil 1999). In the experiments, $n \sim 10^7\,\mathrm{cm}^{-3}$, B runs from 1–4 Tesla, and T could be varied over the range $0.03\mathrm{eV} < T < 3\mathrm{eV}$. For such plasmas, the Debye length is greater than the cyclotron radius so transport due to long range collisions is an important effect.

Exercise 16.3 Show that the maximum possible density (called the Brillouin density n_B) is related to the magnetic field by

$$n_B = m\Omega_c^2/8\pi e^2,$$

and find n_B for Mg^+ ions in a 1 Tesla magnetic field.

In order to measure diffusion across the magnetic field lasers are used to tag some of the ions via their spins. First, a laser directed across the column intersects all ions as the plasma rotates and pumps them all into the $s_z = +1/2$ spin state. This beam is then turned off and a second "tagging" beam, directed along the trap axis, pumps ions in the beam into the $s_z = -1/2$ state. This can be done very quickly compared to the rate at which particles diffuse out of the beam. After this tagging beam is turned off, the $s_z = -1/2$ ions (the "test particles") diffuse across the magnetic field. A weak probe beam that does not change the spin is then used to measure the density $n_t(r,t)$ of the test particles, through their fluorescence in the probe beam. Given $n_t(r,t)$, one can obtain the radial test particle flux Γ_r through the continuity equation,

$$\frac{\partial n_t}{\partial t} = -\frac{1}{r}\frac{\partial}{\partial r}(r\Gamma_r), \tag{16.40}$$

which implies

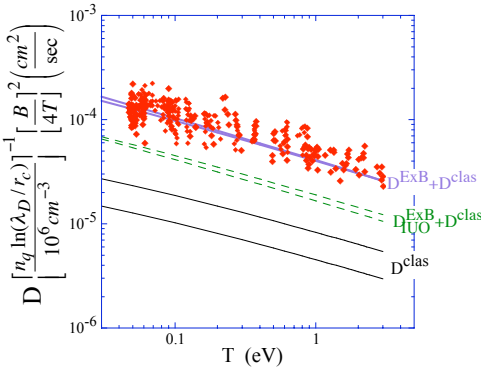

Fig. 16.5 Measured test particle diffusion compared to eqn (16.37) (dashed lines), the classical theory (lower solid lines), and the improved theory discussed in Section 2.3 (upper solid lines) [from Anderegg (1997)].

$$\Gamma_r(r,t) = \int_{\infty}^{r} r' dr' \frac{\partial n_t}{\partial t}(r',t). \tag{16.41}$$

We compare Γ_r to Fick's law, which states that in a diffusive process the flux of test particles is proportional to the gradient in their concentration:

$$\Gamma_r = -Dn\frac{\partial}{\partial r}\left(\frac{n_t}{n}\right). \tag{16.42}$$

Note that while n_t diffuses, n remains fixed since the plasma is in equilibrium. Rather, the concentration of test particles eventually becomes uniform. Also, experiments were performed on near-thermal-equilibrium plasmas which rotate rigidly, so we assume that $v_{\min}$ is set by collisions, not flow shear.

The experimentally-determined values of Γ_r are found to be proportional to $n\,\partial/\partial r\,(n_t/n)$, and their ratio yields D. Results for D using this method are displayed in Fig. 16.5 versus plasma temperature for a range of magnetic field strengths and densities. The figure shows that the measured diffusion is roughly 10 times the classical theory prediction from Table 16.1, but is also about 3 times the prediction of eqn (16.37) for $\mathbf{E}\times\mathbf{B}$ drift collisions. Evidently the theory presented so far requires modification.

16.2.3 Correction to Integration Along Unperturbed Orbits

The IUO technique used in deriving eqn (16.37) gives a diffusion coefficient which is up to three times too small because of a subtle "collisional caging" effect. To understand this, we will start the calculation over again using a slightly different approach, based on the Green-Kubo expression for spatial diffusion,

$$D = \frac{1}{2}\left(\frac{c}{B}\right)^2 \int_{-\infty}^{\infty} dt \langle E_y(t) E_y(0)\rangle \tag{16.43}$$

where $E_y(t)$ is the fluctuating electric field acting on a test particle, labeled "1," due to its collisions with other particles as they stream by. This fluctuating field

creates a fluctuating velocity $v_x(t) = cE_y/B$ that is responsible for the diffusion in x. Equation (16.43) can be derived from the equation of motion $dx/dt = v_x(t)$, which implies

$$\langle x^2\rangle(t) = \int_0^t dt'dt''\langle v_x(t')v_x(t'')\rangle. \tag{16.44}$$

The derivation relies on three assumptions: (1) $\langle v_x(t')v_x(t'')\rangle$ is a function only of $t'-t''$ (the fluctuating velocities are stationary); (2) this correlation function approaches zero for $|t'-t''| > \tau$ (the "autocorrelation time"); and (3) times of interest satisfy $t \gg \tau$. Using these assumptions, it is not difficult to show that $\langle x^2\rangle = 2Dt$ with D given by eqn (16.43) (Reif 1965).

The electric field in eqn (16.43) can be expressed as a Fourier transform:

$$E_y(t) = -\sum_{j=2}^{N} e\int \frac{d^3k}{(2\pi)^3}\frac{4\pi e i k_y}{k^2}e^{i\mathbf{k}\cdot\Delta\mathbf{r}_j(t)} \tag{16.45}$$

where $\Delta\mathbf{r}_j(t) = \mathbf{r}_1(t) - \mathbf{r}_j(t)$ is the difference between the test particle position and that of particle j. Their relative position evolves according to

$$\Delta\mathbf{r}_j(t) = \Delta\mathbf{r}_j(0) + \hat{z}v_r t + \tilde{z}_r(t), \tag{16.46}$$

where v_r is the initial relative velocity, and $\tilde{z}_r(t)$ is the fluctuating relative position change caused by collisions:

$$d^2\tilde{z}_r/dt^2 = eE_z(t)/m, \tag{16.47}$$

where $E_z(t)$ is a fluctuating electric field due to interactions with the plasma.

Exercise 16.4 Show that

$$\langle e^{ik_z\tilde{z}_r(t)}\rangle = e^{-k_z^2 D_v|t|^3/3} \tag{16.48}$$

where $D_v = (e/m)^2\int_0^\infty dt'\langle E_z(t')E_z(0)\rangle$ is the velocity diffusion coefficient, assuming that $t \gg \tau$ where τ is the autocorrelation time for the fluctuations in $E_z(t)$.

Equation (16.43) then becomes

$$D = \frac{1}{2}\left(\frac{ce}{B}\right)^2\sum_{j=2}^{N}\sum_{\ell=2}^{N}\int_{-\infty}^{\infty}dt\int\frac{d^3kd^3k'}{(2\pi)^6}\frac{(4\pi i)^2k_yk'_y}{k^2k'^2}\langle e^{i\mathbf{k}\cdot\Delta\mathbf{r}_j(t)+i\mathbf{k}'\cdot\Delta r_\ell(0)}\rangle. \tag{16.49}$$

In order to evaluate the average, we assume that initial conditions for the particles are uncorrelated, so that the probability distribution for these initial conditions is a product of the distribution function for each separate charge. Also, we *assume* that the fluctuations in $E_z(t)$ are uncorrelated from the initial conditions, so that

$$\langle e^{i\mathbf{k}\cdot\Delta\mathbf{r}_j(t)+i\mathbf{k}'\cdot\Delta r_\ell(0)}\rangle = \langle e^{i\mathbf{k}\cdot(\Delta r_j(0)+v_rt)+i\mathbf{k}'\cdot\Delta\mathbf{r}_\ell(0)}\rangle \times e^{-k_z^2D_v|t|^3/3}. \tag{16.50}$$

It is then not difficult to show that

$$\langle \sum_j \sum_\ell e^{i\mathbf{k}\cdot\Delta\mathbf{r}_j(0)+i\mathbf{k}'\cdot\Delta\mathbf{r}_\ell(0)}\rangle = \frac{N-1}{V}\int d^3\Delta r_j(0)\int dv_r f_{\rm rel}(v_r) \times e^{i(\mathbf{k}+\mathbf{k}')\cdot\Delta\mathbf{r}_j(0)} = n(2\pi)^3\delta(\mathbf{k}+\mathbf{k}')\int dv_r f_{\rm rel}(v_r). \tag{16.51}$$

Applying this expression to eqn (16.49) and performing the $\mathbf{k}'$ integral, the diffusion coefficient may be expressed as

$$D = \frac{(4\pi)^2}{2}\left(\frac{ce}{B}\right)^2 n\int_{-\infty}^{\infty} dv_r f_{\rm rel}(v_r)\int \frac{d^3k}{(2\pi)^3}\frac{k_y^2}{k^4}\int_{-\infty}^{\infty} dt\, e^{ik_z v_r t - k_z^2 D_v|t|^3/3}. \tag{16.52}$$

We write d^3k in cylindrical coordinates $(k_\perp, \theta, k_z)$, and define $\bar{k}_z = k_z/k_\perp$ and $\bar{t} = k_\perp v_r t$. Then eqn (16.52) can be written as

$$D = \left(\frac{ce}{B}\right)^2 n\int_{-\infty}^{\infty} dv_r \frac{e^{-mv_r^2/4T}}{\sqrt{4\pi T/m}}\int_0^\infty k_\perp dk_\perp \frac{1}{k_\perp^2|v_r|}\int_{-\infty}^{\infty} d\bar{t} J(\bar{D}_v,\bar{t}) \tag{16.53}$$

where $\bar{D}_v = D_v/(3k_\perp v_r^3)$ and

$$J(\bar{D}_v,\bar{t}) = \int_{-\infty}^{\infty}\frac{d\bar{k}_z}{(1+\bar{k}_z^2)^2}\, e^{i\bar{k}_z\bar{t}-\bar{k}_z^2\bar{D}_v|\bar{t}|^3}. \tag{16.54}$$

This function is plotted versus $\bar{t}$ in Fig. 16.6.

We require the integral over $\bar{t}$ of J in the expression for D, eqn (16.53). The result of this integration depends on the value of $\bar{D}_v$. For $\bar{D}_v = 0$, it is clear that

$$\int_{-\infty}^{\infty} d\bar{t}\, J(0,\bar{t}) = 2\pi \tag{16.55}$$

since $\int_{-\infty}^{\infty} d\bar{t} e^{i\bar{k}_z\bar{t}} = 2\pi\delta(\bar{k}_z)$. This result, together with imposition of the appropriate cutoffs, leads back to eqn (16.37), as expected since $\bar{D}_v = 0$ is equivalent to the integration along unperturbed orbits. On the other hand, when $\bar{D}_v \neq 0$, but $\bar{D}_v \to 0$, one can show the following:

$$\lim_{\bar{D}_v\to 0^+}\int_{-\infty}^{\infty} d\bar{t}\, J(\bar{D}_v,\bar{t}) = 6\pi \tag{16.56}$$

This is *3 times* the result one obtains for $\bar{D}_v$ identically equal to zero (Dubin 1997).

Exercise 16.5 Verify eqn (16.56). (Hint: transform variables. See Dubin (1997) for details.)

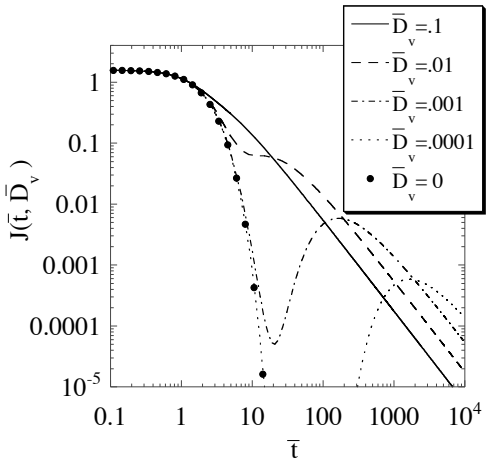

Fig. 16.6 The function $J(\bar{D}_v, \bar{t})$.

Even an infinitesimal amount of velocity diffusion makes a large change to the result for D, increasing it by a factor of 3. Equation (16.56) can be verified by numerical integration, and the result is displayed in Fig. 16.7. Note that as $v_r \to 0$, $\bar{D}_v \to \infty$ because $\bar{D}_v = D_v/3k_\perp v_r^3$. Also, Fig. 16.7 shows that for $\bar{D}_v \gtrsim 1$, $\int_{-\infty}^{\infty} J(\bar{D}_v, t)dt \to 0$. This provides a natural cutoff to the logarithmically divergent v_r integral in eqn (16.53) at $v_{\min} \sim (D_v/3k_\perp)^{1/3}$. This is the same minimum velocity as used in deriving eqn (16.37), but expressed in k-space. Then after performing the v_r integral to logarithmic order, eqn (16.53) becomes:

$$D = \frac{6\sqrt{\pi}}{\bar{v}} \left(\frac{ce}{B}\right)^2 n \int_0^\infty \frac{dk_\perp}{k_\perp} \ln\left(\frac{\bar{v}}{(D_v/3k_\perp)^{1/3}}\right). \tag{16.57}$$

Next, the logarithmic divergence in $k_\perp$ is cut off at λ_D^{-1} and r_c^{-1} for the same reasons as we cut off the ρ integral in eqn (16.35), resulting in

$$D = 3D_{\rm IUO} \tag{16.58}$$

where $D_{\rm IUO}$ is the result of integration along unperturbed orbits ($\bar{D}_v = 0$), given by eqn (16.37).

Integration along unperturbed orbits fails to capture the extra factor of 3 because when $\bar{D}_v = 0$, as assumed in IUO, particles only collide once as they pass one another along the magnetic field. However, when $\bar{D}_v$ is small but finite, particles encounter one another many times as their relative velocities diffuse: eventually, particle velocities reverse and the pair collides again. Effectively, collisions with surrounding particles (responsible for the velocity diffusion) cause a colliding pair to interact over a longer period of time than would occur in the absence of collisions (this is the "collisional caging" effect referred to at the beginning of the section: surrounding particles "cage" the interacting pair). This longer interaction time can be seen directly in the plot of

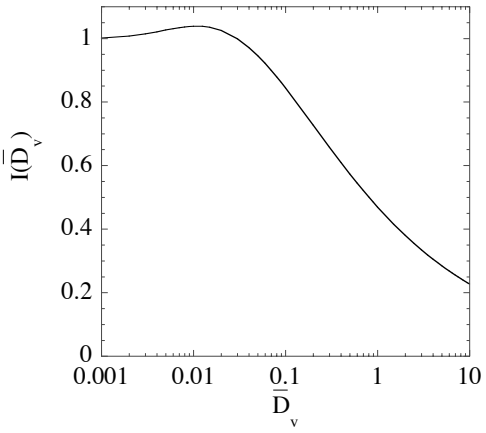

Fig. 16.7 The function $I(\bar{D}_v) \equiv \frac{1}{6\pi}\int_{-\infty}^{\infty} J(\bar{D}_v, \bar{t})d\bar{t}$.

$\bar{J}(\bar{D}_v, \bar{t})$ versus time, in Fig. 16.6. For $\bar{D}_v = 0$, $\bar{J}$ displays a single peak at $\bar{t} = 0$, due to the single collision. However for $\bar{D}_v$ small but finite, a second peak appears, caused by further collisions between the pair as their diffusing relative velocity changes sign. This peak occurs at $\bar{t} \sim 0.1/\bar{D}_v$. These multiple collisions are responsible for the increase (by a factor of 3) of the diffusion D.

Another way to think of the factor of 3 increase is that our estimate $v_{\min} \sim (D_v\rho)^{1/3}$ was incorrect. One can rewrite $3\ln(\bar{v}/(D_v\rho)^{1/3})$ as $\ln(\bar{v}/v'_{\min})$ where $v'_{\min} = \nu\rho$ is an improved estimate for the minimum relative velocity. This is much smaller than $(D_v\rho)^{1/3}$, and comes about because particles interact for a much longer time than our previous estimate suggested–see Fig. 16.6.

Returning now to the effect of fluid shear on the transport, we note that shear will supercede collisions when $S > \nu$, so that $v_{\min} = S\rho$ rather than $\nu\rho$. Accounting for fluid shear then yields

$$D = 2\sqrt{\pi}\,\nu_0 r_c^2 \ln\left(\frac{\lambda_D}{r_c}\right) \ln\left(\frac{\bar{v}}{\mathrm{Max}(S,\nu)\sqrt{\lambda_D r_c}}\right). \tag{16.59}$$

Equation (16.59) can be verified by including fluid shear from the beginning in the previous diffusion calculation; however the details are too complex to include here. One portion of the calculation is considered in exercise 16.6. Also, in a previous description of the effect of fluid shear on diffusion (Driscoll *et al.* 2002), a multiplicative parameter α was introduced to account for the enhancement factor. Equation (16.59) is equivalent to that description since the enhancement is included through use of our improved estimate for the minimum relative velocity.

In comparing theory to experiment we assume $S < \nu$ since the plasmas are near thermal equilibrium, rotating rigidly. Figure 16.6 shows the experiments compared to the improved theory of eqn (16.58), or equivalently, (16.59).

Exercise 16.6 Derive eqn (16.59) for the case $\bar{D}_v = 0$ (i.e. $v_{\min}$ determined by shear) by repeating the analysis that leads to (16.58), but setting $\tilde{z}_r = 0$ in eqn (16.46) and keeping shear, replacing the equation by $\Delta\mathbf{r}_j(t) = \Delta\mathbf{r}_j(0) + \hat{z}v_r t + \hat{y}S\Delta x t$.

16.3 Heat Conduction across B

In this lecture we consider the problem of heat conduction across a strong magnetic field, in a plasma for which $\bar{r}_c \ll \lambda_D$. Following Psimopolis and Li (1992), we employ an approach based on an ad hoc generalization of the Boltzmann collision operator that describes isolated two-particle collisions. Weaknesses in this approach will become apparent, but it has the advantage of being quite straightforward, and it points out the necessity of deriving a new collision operator that is capable of properly handling long-range interactions.

Based on the estimate discussed in Lecture 1, we consider a picture of collisions as shown in Fig. 16.3: 2 particles on field lines separated by $\rho \sim \lambda_D$ interact as they pass by one another. Initially, their parallel velocities are v_{z_1} and v_{z_2} respectively. After their interaction their velocities are v'_{z_1} and v'_{z2}. The change in kinetic energies of each particle results in transfer of energy across $\mathbf{B}$.

In such a one-dimensional collision, relative energy E_r of the two particles is conserved:

$$E_r = \frac{mv_r^2}{4} + \frac{e^2}{(\rho^2 + z_r^2)^{1/2}} \tag{16.60}$$

where $z_r = z_1 - z_2$ is the relative position. This implies that the initial and final relative speeds are the same: $|v_r| = |v'_r|$. However, the sign of v_r can change. If, initially (when $z_r \gg \rho$),

$$\frac{mv_r^2}{4} < \frac{e^2}{\rho} \tag{16.61}$$

the repulsive Coulomb potential will cause the particles to reflect from one another so that $v'_r = -v_r$. If, on the other hand, inequality (16.61) is not satisfied, the relative energy is sufficient to overcome the repulsion and particles do not reflect so that $v'_r = v_r$. Combining these results with momentum conservation, $v_{z_1} + v_{z_2} = v'_{z_1} + v'_{z_2}$, we find that when inequality (16.61) is satisfied

$$v'_{z_1} = v_{z_2} \text{ and } v'_{z_2} = v_{z_1} \tag{16.62}$$

i.e. particles exchange velocities; if eqn (16.61) is not satisfied their velocities are unchanged by the interaction.

Now, consider the effect that these interactions have on a distribution of particles $f(x_1, v_{z_1}, t)$, described by a Maxwellian with varying temperature $T(x_1, t)$:

$$f(x_1, v_{z_1}, t) = \frac{n\, e^{-mv_{z_1}^2/2T(x_1,t)}}{\sqrt{2\pi T(x_1,t)/m}}. \tag{16.63}$$

In a Boltzmann picture (Lifshitz and Pitaevskii 1981), the number of particles in element dv_{z_1} at position x_1, $f(x_1, v_{z_1}, t)dv_{z_1}$, varies in time as collisions remove

particles from this element, and other collisions introduce particles into the element. The rate of removal is the number of particles in dv_{z_1}, $f(x_1, v_{z_1})dv_{z_1}$, multiplied by the total number of collisions per unit time,

$$\int dx_2 dy_2 \int dv_{z_2} |v_r| f(x_2, v_{z_2}, t), \tag{16.64}$$

where $v_r = v_{z_1} - v_{z_2}$, and the integral over x_2 and y_2 must satisfy eqn (16.61); otherwise there is no change in the velocities due to the interaction. Similarly, the rate at which collisions introduce particles into the element is

$$dv_{z_1} \int dx_2 dy_2 \int dv_{z_2} |v_r| f(x_1, v_{z_2}, t) f(x_2, v_{z_1}, t), \tag{16.65}$$

since particles that begin at velocity v_{z_2} will end up with velocity v_{z_1} in a collision with a particle moving at that velocity. Taking the difference between these two rates yields the overall rate of change of $f(x_1, v_{z_1})$:

$$\begin{aligned} \frac{d}{dt} f(x_1, v_{z_1}, t) = \int dx_2 dy_2 \int_{m v_r^2/4 < e^2/\rho} dv_{z_2} |v_r| \\ \times (f(x_1, v_{z_2}, t) f(x_2, v_{z_1}, t) - f(x_1, v_{z_1}, t) f(x_2, v_{z_2}, t)). \end{aligned} \tag{16.66}$$

The right-hand side is similar in form to the Boltzmann collision operator, except that the distribution functions are evaluated at *different* points in space, x_1 and x_2. This is important in order to describe heat conduction caused by energy-transferring collisions.

The rate of change of temperature may now be found by integrating eqn (16.66) over $m v_{z_1}^2$, and substituting for f from eqn (16.63):

$$\begin{aligned} \frac{\partial T}{\partial t}(x_1, t) &= \frac{1}{n} \int dv_{z_1} m v_{z_1}^2 \frac{\partial f}{\partial t}(x_1, v_{z_1}, t) \\ &= \int dx_2 dy_2 \int_{m v_r^2/4 < e^2/\rho} dv_{z_1} dv_{z_2} \frac{|v_r| m^2 n v_{z_1}^2}{2\pi \sqrt{T_1 T_2}} \\ &\quad \times [e^{-m(v_{z_2}^2/T_1 + v_{z_1}^2/T_2)/2} - e^{-m(v_{z_1}^2/T_1 + v_{z_2}^2/T_2)/2}] \end{aligned} \tag{16.67}$$

where $T_1 = T(x_1, t)$ and $T_2 = T(x_2, t)$.

By interchanging the dummy variables v_{z_1} and v_{z_2}, eqn (16.67) can be expressed as

$$\frac{\partial T_1}{\partial t} = \int dx_2 \, F(x_1, x_2, t) \tag{16.68}$$

where the function F is odd under interchange of x_1 and x_2:

$$\begin{aligned} F(x_1, x_2, t) = \int dy_2 \int dv_{z_1} dv_{z_2} \frac{|v_r| m^2 n}{4\pi \sqrt{T_1 T_2}} (v_{z_1}^2 - v_{z_2}^2) \\ \times [e^{-m(v_{z_2}^2/T_1 + v_{z_1}^2/T_2)/2} - e^{-m(v_{z_1}^2/T_1 + v_{z_2}^2/T_2)/2}]. \end{aligned} \tag{16.69}$$

Since $F(x_1, x_2, t)$ is odd under interchange of x_1 and x_2, we will write it as

$$F(x_1, x_2, t) = \bar{F}(X, x_r, t) \tag{16.70}$$

where $X = (x_1 + x_2)/2$, $x_r = x_2 - x_1$, and $\bar{F}$ is odd in x_r (i.e. $\bar{F} \to -\bar{F}$ as $x_r \to -x_r$). This transformation implies that

$$x_1 = X - x_r/2 \ , \ x_2 = X + x_r/2. \tag{16.71}$$

Then

$$\int dx_2 F(x_1, x_2, t) = \int dx_2 \bar{F}(\frac{x_1 + x_2}{2}, x_2 - x_1, t) \tag{16.72}$$

and converting the integration variable to x_r we obtain

$$\int dx_2 F = \int dx_r \bar{F}(x_1 + \frac{x_r}{2}, x_r). \tag{16.73}$$

We now assume that values of x_r required in eqn (16.68) are small (of order λ_D) compared to the scale of variation of $T(x_1, t)$, so that we may Taylor expand $\bar{F}$ in the first argument, obtaining

$$\int dx_2 F = \int dx_r \bar{F}(x_1, x_r, t) + \frac{\partial}{\partial x_1} \int dx_r \frac{x_r}{2} \bar{F}(x_1, x_r, t). \tag{16.74}$$

The first integral vanishes because $\bar{F}$ is odd in x_r. Converting $\bar{F}$ back to F using eqn (16.70) and (16.71) yields

$$\frac{\partial T_1}{\partial t} = \frac{\partial}{\partial x_1} \int dx_r \frac{x_r}{2} F(x_1 - \frac{x_r}{2}, x_1 + \frac{x_r}{2}, t). \tag{16.75}$$

Substituting for F from eqn (16.69) and Taylor expanding $T(x_1 \pm x_r/2, t)$, to first order in x_r, we obtain the heat equation:

$$\frac{\partial T_1}{\partial t} = \frac{\partial}{\partial x_1}(\chi \frac{\partial T_1}{\partial x_1}) \tag{16.76}$$

where the thermal diffusivity χ is given by the expression

$$\chi = \int dx_2 dy_2 \int_{m v_r^2/4 < e^2/\rho} dv_{z_1} dv_{z_2} \frac{x_r^2}{2} \frac{|v_r| m^3 n}{8\pi T_1^3} (v_{z_1}^2 - v_{z_2}^2)^2 e^{-m(v_{z_1}^2 + v_{z_2}^2)/2T_1}. \tag{16.77}$$

The integrals over velocity can be most easily performed by converting to relative and center of mass variables, and the result is

$$\chi = \frac{1}{\pi} n \bar{v} b^2 \int dx_2 dy_2 \frac{x_r^2}{\rho^2}. \tag{16.78}$$

Exercise 16.7 Derive eqn (16.78) from eqn (16.77).

Converting to polar coordinates for which $dx_2 dy_2 = \rho d\rho d\theta$, and $x_r = \rho\cos\theta$, we can perform the θ integral in eqn (16.78), yielding

$$\chi = \sqrt{\pi} n \bar{v} b^2 \int_0^\infty \rho d\rho. \tag{16.79}$$

This result is clearly divergent at large impact parameters. The range of impact parameters must be cut off due to Debye shielding, so we take $\rho_{\max} = \lambda_D$, yielding

$$\chi = \sqrt{\pi}/2\, n \bar{v} b^2 \lambda_D^2. \tag{16.80}$$

Note however that unlike previous logarithmic divergences, a change in $\rho_{\max}$ by a factor of 2 causes a large change in χ, by a factor of 4. Thus, eqn (16.80) can only be regarded as an estimate; the numerical coefficient is unknown. Furthermore, our treatment of collisions as isolated two-body events breaks down at impact parameters of order λ_D, since many other particles surrounding the colliding pair intervene. This approach, while a useful exercise, points to the need for a proper derivation of a collision operator to replace eqn (16.66); one which can rigorously describe the effect of long range interactions without assuming they consist of isolated two-body collisional events. This will be the topic of lecture 4.

16.4 Collision Operator for Long-Range Interactions

In this lecture we will derive a new collision operator that describes collisional interactions between particles separated by a Debye length or more in a plasma for which $\bar{r}_c \ll \lambda_D$.

16.4.1 Plasma Response to a Moving Charge

As a first step we will examine the response of a magnetized plasma to a moving charge Q with velocity $v_0\hat{z}$ along the magnetic field $B\hat{z}$. Previously we analyzed how a plasma responds to a stationary charge by Debye-shielding the charge. When the charge is moving the plasma response is more complicated: the possibility exists that the charge will emit plasma waves. This response should be an integral component of our collision operator, since the operator must describe interactions between moving charges, including the self-consistent plasma response.

The moving charge creates a potential disturbance $\delta\phi(\mathbf{r}, t)$ that follows from Poisson's equation:

$$\nabla^2 \delta\phi = -4\pi e \int \delta f dv_z - 4\pi Q \delta(\mathbf{r} - v_0 \hat{z} t), \tag{16.81}$$

where $\delta f(\mathbf{r}, v_z, t)$ is the perturbation away from the equilibrium distribution function $f_0(v_z)$. This perturbation can be obtained by solving the guiding-center Vlasov equation

$$\frac{\partial f}{\partial t} + v_z \frac{\partial f}{\partial z} + \frac{e}{m} E_z \frac{\partial f}{\partial v_z} = 0. \tag{16.82}$$

Here we assume for simplicity that B is very large so only motion along z is needed, and we neglect cyclotron motion and $\mathbf{E} \times \mathbf{B}$ drifts (Chen 1974). Linearizing the equation in $\delta\phi$, taking $\delta f = f - f_0$ we obtain the linearized Vlasov equation

$$\frac{\partial \delta f}{\partial t} + v_z \frac{\partial \delta f}{\partial z} - \frac{e}{m} \frac{\partial \delta \phi}{\partial z} \frac{\partial f_0}{\partial v_z} = 0. \tag{16.83}$$

We will solve eqns. (16.81) and (16.83) for $\delta\phi(\mathbf{r}, t)$ via a Fourier Laplace transform, writing

$$\delta\phi(\mathbf{r}, t) = \int \frac{d^3k}{(2\pi)^3} \int_C \frac{dp}{2\pi i} e^{i\mathbf{k}\cdot\mathbf{r}+pt} \delta\phi_{\mathbf{k}p} \tag{16.84}$$

where $\delta\phi_{\mathbf{k}p}$ is the Fourier-Laplace amplitude, and the contour C runs from $-i\infty$ to $i\infty$, to the right of any poles in $\delta\phi_{\mathbf{k}p}$. Applying the Fourier-Laplace transform to eqn (16.83) yields

$$(p + ik_z v_z)\delta f_{\mathbf{k}p} - \frac{e}{m} ik_z \delta\phi_{\mathbf{k}p} \frac{\partial f_0}{\partial v_z} = \delta f_{\mathbf{k}}(t = 0), \tag{16.85}$$

where $\delta f_{\mathbf{k}}(t = 0)$ is the Fourier transform of $\delta f(\mathbf{r}, t = 0)$. We assume that initially the plasma is unperturbed so $\delta f_{\mathbf{k}}(t = 0) = 0$. Then solving eqn (16.85) for $\delta f_{\mathbf{k}p}$ and substituting the result into the Fourier-Laplace transform of eqn (16.81),

$$-k^2 \delta\phi_{\mathbf{k}p} = -4\pi e \int dv_z \delta f_{\mathbf{k}p} - \frac{4\pi Q}{p + ik_z v_0} \tag{16.86}$$

yields the following expression for $\delta\phi_{\mathbf{k}p}$,

$$\delta\phi_{\mathbf{k}p} = \frac{4\pi Q}{k^2 D_{\mathbf{k}p}} \frac{1}{p + ik_z v_0}, \tag{16.87}$$

where $D_{\mathbf{k}p}$ is the *linear plasma dieletric function*:

$$D_{\mathbf{k}p} = 1 - \frac{4\pi e^2 ik_z}{mk^2} \int dv_z \frac{\partial f_0/\partial v_z}{p + ik_z v_z}. \tag{16.88}$$

This function describes the shielding response of the plasma. As written, eqn (16.88) is correct only for $\mathrm{Re}(p) > 0$ since the Laplace transform contour C must run to the right of all singularities, and the v_z integral in eqn (16.88) is singular at $\mathrm{Re}(p) = 0$. For $\mathrm{Re}(p) \leq 0$, eqn (16.88) must be analytically continued: the v_z integration contour must be deformed below the real line in the complex v_z plane, so that p remains above the v_z integration contour (Krall and Trivelpiece 1986).

Equation (16.87) must now be substituted in eqn (16.84) to obtain $\delta\phi(\mathbf{r}, t)$. The inverse Laplace transform in eqn (16.84) has two types of poles in the integrand: zeroes in $D_{\mathbf{k}p}$ and the pole at $p = -ik_z v_0$. We will assume that all zeroes at $D_{\mathbf{k}p}$ are damped, i.e. these zeroes are at $Re\, p < 0$, so that they produce a time-dependent response in $\delta\phi$ that damps away, giving no contribution at large times. The undamped pole, at $p = -ik_z v_0$, yields

$$\delta\phi(\mathbf{r}, t) = 4\pi Q \int \frac{d^3k}{(2\pi)^3} \frac{e^{i\mathbf{k}\cdot\mathbf{r}-ik_z v_0 t}}{k^2 D_{\mathbf{k},-ik_z v_0+\varepsilon}} \tag{16.89}$$

where ε is a positive infinitesimal used to ensure that the integration in p has passed to the right of singularities in $D_{\mathbf{k}p}$ (this is equivalent to deforming the v_z integration

contour below the pole at $v_z = v_0$). Equation (16.89) implies that $\delta\phi = \delta\phi(x, y, z - v_0 t)$, i.e. the potential is a stationary perturbation as seen in the frame of the moving charge.

In order to complete our examination of the plasma response to the moving charge, we need to understand the plasma dielectric function $D_{\mathbf{k},ik_z v_0+\varepsilon}$. This function clearly depends on the velocity v_0 of the charge. If $v_0 = 0$, eqn (16.88) implies

$$D_{\mathbf{k},0} = 1 - \frac{4\pi e^2}{mk^2} \int \frac{dv_z}{v_z} \frac{\partial f_0}{\partial v_z}. \tag{16.90}$$

If f_0 is given by a Maxwellian distribution, $\partial f_0/\partial v_z = -v_z f_0/\bar{v}^2$, and eqn (16.90) yields

$$D_{\mathbf{k},0} = 1 + \frac{1}{k^2\lambda_D^2}, \tag{16.91}$$

the dielectric response for static Debye shielding. Using this in eqn (16.89) leads to $\delta\phi(\mathbf{r}, t) = Qe^{-r/\lambda_D}/r$, as expected for Debye shielding of a stationary charge due to a single plasma species.

For $v_0 \neq 0$, the plasma response is more complicated. Defining $\omega = k_z v_0$, and again assuming that f_0 is given by a Maxwellian, the dielectric function can be written as

$$D_{\mathbf{k},-i\omega+\varepsilon} = 1 + \frac{k_z}{k^2\lambda_D^2} \int_{-\infty}^{\infty} dv_z f_{\max}(v_z) \frac{v_z}{k_z v_z - \omega - i\varepsilon}. \tag{16.92}$$

Since $\omega = k_z v_0$ is real and ε is a positive infinitesimal we can use the Plemelj formula to break the integral into a principal part and an imaginary contribution from the pole at $\omega = k_z v_z - i\varepsilon$:

$$\begin{aligned} D_{\mathbf{k},-i\omega+\varepsilon} &= 1 + \frac{k_z}{k^2\lambda_D^2} \left[\int\!\!\!\!\!\!-_{-\infty}^{\infty} dv_z \frac{f_{\max}(v_z)}{k_z v_z - \omega} + i\pi \int_{-\infty}^{\infty} dv_z f_{\max}(v_z) v_z \delta(k_z v_z - \omega) \right] \\ &= 1 + \frac{1}{k^2\lambda_D^2} \left[a\left(\frac{v_0}{\bar{v}}\right) + ib\left(\frac{v_0}{\bar{v}}\right) sgn(k_z) \right] \end{aligned} \tag{16.93}$$

where the real functions $a(x)$ and $b(x)$ are defined as

$$a(x) \equiv \int\!\!\!\!\!\!-_{-\infty}^{\infty} \frac{ds}{\sqrt{2\pi}} \frac{se^{-s^2/2}}{s - x}\ ,\ b(x) \equiv \sqrt{\frac{\pi}{2}} xe^{-x^2/2}. \tag{16.94}$$

Then the potential surrounding the charge is found by substituting eqn (16.93) in eqn (16.89).

Exercise 16.8 Show that $\delta\phi(x, y, z - v_0 t)$ can be written as

$$\delta\phi = \frac{Q}{r} g\left(\frac{\rho}{\lambda_D}, \frac{z - v_0 t}{\lambda_D}\right) \tag{16.95}$$

where $\rho^2 = x^2 + y^2$, $r^2 = z^2 + \rho^2$, and the shielding function $g(\rho, z)$ is

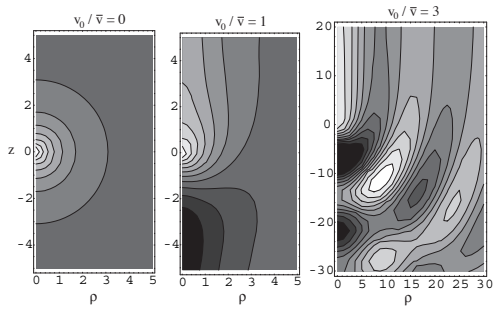

Fig. 16.8 Contour plots of the shielding function $g(\rho, z)$ at $v_0/\bar{v} = 0$, 1 and 3.

$$g(\rho, z) = \frac{2}{\pi} r\, Re\left[\int_0^\infty k_\perp dk_\perp J_0(k_\perp \rho) \int_0^\infty dk_z \frac{e^{ik_z z}}{k_z^2 + k_\perp^2 + a(v_0/\bar{v}) + ib(v_0/\bar{v})}\right]. \tag{16.96}$$

(Hint: Evaluate eqn (16.89) in cylindrical coordinates, scaling $\mathbf{k}$ to the Debye length.)

The shielding function is plotted in Figs. 16.8 and 16.9 for several values of the particle speed v_0. At $v_0 = 0$ the static Debye shielding response is evident; $g(\rho, z) = e^{-\sqrt{\rho^2+z^2}}$. However, for $v_0 \neq 0$ the dynamical shielding is incomplete, and as v_0 increases beyond $v_0/\bar{v} \sim 2 - 3$ a damped wave develops behind the moving charge. This wave is due to weakly damped plasma waves that are resonant with the particle: i.e. waves whose phase velocity in the z-direction, ω/k_z, matches the speed v_0 of the particle. Such resonant waves are strongly excited by passage of the particle.

Exercise 16.9 Taking $v_0 = \omega/k_z$ in eqn (16.93) and assuming $v_0 \gg \bar{v}$, show that D is approximately

$$D_{\mathbf{k},-i\omega+\varepsilon} \simeq 1 - \frac{\omega_p^2 k_z^2}{\omega^2 k^2} + \frac{ib\, sgn(k_z)}{k^2 \lambda_D^2}. \tag{16.97}$$

Mathematically, the waves are excited by near-zeros in $D_{\mathbf{k},-i\omega+\varepsilon}$, which provide a large contribution to the integral in eqn (16.89). A near zero in D exists for $\omega/k_z \gg \bar{v}$, at

$$\omega^2 \cong \frac{\omega_p^2 k_z^2}{k^2}, \tag{16.98}$$

(see Exercise 16.9) which is the dispersion relation for magnetized plasma waves. Note that the small imaginary term in eqn (16.97) yields a negative imaginary part to ω, causing the waves to slowly damp. This is the origin of the wavelike response to the passage of the particle when $v_0 \gg \bar{v}$. These waves, a form of Cerenkov radiation, are similar to the wake observed behind a moving boat. They carry energy and momentum away from the particle, which can be reabsorbed by particles a great distance away. This has important consequences for plasma thermal conduction and viscosity, as we will see.

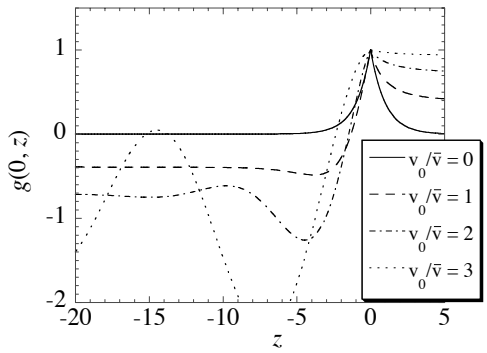

Fig. 16.9 Plot of $g(0,z)$ for $v_0/\bar{v} = 0$, 1, 2 and 3.

Equation (16.95) can also be used to determine the drag force on the moving charge due to the plasma. By subtraction of the bare Coulomb potential $Q/|r|$ from eqn (16.95), the remaining potential $\delta\phi_p(\rho, z - v_0 t)$ can be obtained. This potential, due to the plasma only, creates a force $F = -\partial\delta\phi_p(0,z)/dz|_{z=0}$ that acts on the moving charge to slow it down. One can show that the force scales as $F \sim -m\nu v_0$ for $v_0/\bar{v} \ll 1$, as one might expect. (The logarithmic divergence in ν [see eqn (16.13)] arises from a large k logarithmic divergence in the derivative with respect to z of the wavenumber integral in eqn (16.96), which must be cut off at $k = b^{-1}$.)

16.4.2 Collision Operator for Long-Range Collisions

We now use what we have learned about the shielding response of a plasma to a moving charge in order to derive the collision operator, including self-consistent plasma shielding effects. We assume a plasma in a uniform magnetic field $B\hat{z}$ with several species of charges with mass m_α, charge e_α, and density $n_\alpha(x)$, where α is a species label (e.g. $\alpha =$ electron, or ion). Each species has a distribution function $f_\alpha(x, v_z, t)$. In the absence of collisions, this distribution would satisfy the guiding-center Vlasov equation

$$\frac{\partial f_\alpha}{\partial t} + v_z \frac{\partial f_\alpha}{\partial z} + \frac{\mathbf{E}_0 \times \hat{z}}{B} c \cdot \nabla f_\alpha + \frac{e_\alpha}{m_\alpha} E_{0_z} \frac{\partial f_\alpha}{\partial v_z} = 0, \tag{16.99}$$

where $\mathbf{E}_0 = -\nabla\phi_0$ is the plasma electric field, given by Poisson's equation,

$$\nabla^2 \phi_0 = -4\pi \sum_\infty e_\alpha \int f_\alpha dv_z. \tag{16.100}$$

Equation (16.99) keeps the $\mathbf{E} \times \mathbf{B}$ drift that was neglected in eqn (16.82), as it is important in determining viscosity and diffusion due to long range collisions.

The assumption that $f_\alpha = f_\alpha(x, v_z, t)$ and $\mathbf{E}_0 = E_0(x,t)\hat{x}$ implies that eqn (16.99) reduces to

$$\frac{\partial f_\alpha}{\partial t} = 0, \tag{16.101}$$

implying that any function of x and v_z alone is an equilibrium solution of eqn (16.99).

Normally, one chooses as an initial condition for eqn (16.99) a smooth function of x and v_z. However in reality the plasma consists of a set of discrete particles. If one therfore chooses as the initial condition,

$$f_\alpha(\mathbf{r}, v_z, t=0) = \sum_{i=1}^{N_\alpha} \delta(\mathbf{r} - \mathbf{r}_i(0))\delta(v_z - v_{z_i}(0)), \tag{16.102}$$

i.e. a series of δ-functions at the N_α discrete positions and velocities of the charges in each species α, the solution to the Vlasov-Poisson system can still be found in principle, but it will contain all the detailed information concerning the microscopic interactions between individual charges.

Exercise 16.10 Show that the solution to eqn (16.99) with initial conditions (16.102) is given by the *Klimontovitch density* $\eta_\alpha(\mathbf{r}, v_z, t)$,

$$\eta_\alpha(\mathbf{r}, v_z, t) = \sum_{i=1}^{N_\alpha} \delta(\mathbf{r} - \mathbf{r}_i(t))\delta(v_z - v_{z_i}(t)), \tag{16.103}$$

where $(\mathbf{r}_i(t), v_{z_i}(t))$ is the phase-space trajectory of the ith particle of species α. [Hint: substitute eqn (16.103) into eqn (16.99).]

As shown in Exercise 16.10, the Klimontovitch density satisfies eqn (16.99) with initial condition (16.102), i.e.,

$$\frac{\partial \eta_\alpha}{\partial t} + v_z \frac{\partial \eta_\alpha}{\partial z} + \frac{\mathbf{E} \times \hat{z}}{B} c \cdot \nabla \eta_\alpha + \frac{e_\alpha}{m_\alpha} E_{z\alpha} \frac{\partial \eta_\alpha}{\partial v_z} = 0 \tag{16.104}$$

where

$$\mathbf{E} = -\nabla \Phi \tag{16.105}$$

and

$$\nabla^2 \Phi = -4\pi \sum_\alpha e_\alpha \int dv_z \eta_\alpha. \tag{16.106}$$

Equation (16.104) is often referred to as the Klimontovitch equation (Krall and Trivelpiece 1986), although the only difference between it and the Vlasov equation is the form of the initial condition. This is a big difference, however, since a smooth Vlasov distribution has a different microscopic form than the N_α particles moving along chaotic trajectories described by the Klimontovitch density $\eta_\alpha(\mathbf{r}, v_z, t)$. The connection between these two pictures of the plasma (smoothed and discrete) may be made by averaging over an ensemble of initial conditions for the discrete particle positions and velocities, *assuming that* each individual particle i in species α has position $\mathbf{r}_i$ and velocity v_{z_i} initially distributed according to a smooth probability density $f_\alpha(x_i, v_{z_i}, t=0)/N_\alpha$.

Then at later times the following function $f_\alpha(x, v_z, t)$ is *defined* by the average over initial conditions:

$$\langle \eta_\alpha(\mathbf{r}, v_z, t) \rangle \equiv f_\alpha(x, v_z, t). \tag{16.107}$$

One may easily show using eqn (16.103) that $\langle \eta_\alpha(\mathbf{r}, v_z, t=0) \rangle = f_\alpha(x, v_z, t=0)$, so eqn (16.107) is consistent with the initial conditions.

The averaged distribution function f_α does not satisfy the Vlasov equation; rather, it evolves slowly in time due to collisions. An equation for f_α can be obtained by applying the above-described averaging procedure to the Klimontovitch equation itself:

$$\frac{\partial f_\alpha}{\partial t} + v_z \frac{\partial f_\alpha}{\partial z} + \langle \frac{\mathbf{E} \times \hat{z}}{B} c \cdot \nabla \eta_\alpha \rangle + \langle \frac{e_\alpha}{m_\alpha} E_{z_\alpha} \frac{\partial \eta_\alpha}{\partial v_z} \rangle = 0. \tag{16.108}$$

It is useful to break $\mathbf{E}$ and η_α into a smooth averaged part and a fluctuation due to discreteness:

$$\eta_\alpha = f_\alpha(x, v_z, t) + \delta\eta_\alpha(\mathbf{r}, v_z, t) \ , \ \mathbf{E} = E_0(x,t)\hat{x} + \delta\mathbf{E}(\mathbf{r}, t). \tag{16.109}$$

Then eqn (16.108) can be written as

$$\frac{\partial f_\alpha}{\partial t} = C_\alpha[\mathbf{f}] \tag{16.110}$$

where the collision operator $C_\alpha[\mathbf{f}]$ is

$$C_\alpha[\mathbf{f}] = -\nabla \cdot \langle \frac{c}{B} \delta\mathbf{E} \times \hat{z} \delta\eta_\alpha \rangle - \frac{\partial}{\partial v_z} \langle \frac{e_\alpha}{m_\alpha} \delta E_z \delta\eta_\alpha \rangle \tag{16.111}$$

and the notation $C_\alpha[\mathbf{f}]$ denotes a functional dependence on f_β for all β. This dependence is implicit in eqn (16.111) through the dependence of the fluctuations $\delta\eta_\alpha$ and $\delta\mathbf{E}$ on f_β, and may be uncovered by subtracting eqn (16.108) from eqn (16.104) to obtain equations for the fluctuations $\delta\eta_\alpha$ and $\delta\mathbf{E}$. If one assumes that the fluctuations are small, one may linearize the resulting equation in the fluctuations to obtain

$$\frac{\partial \delta\eta_\alpha}{\partial t} + v_z \frac{\partial \delta\eta_\alpha}{\partial z} + V_y \frac{\partial \delta\eta_\alpha}{\partial y} + \frac{\delta E_y c}{B} \frac{\partial f_\alpha}{\partial x} + \frac{e_\alpha}{m_\alpha} \delta E_z \frac{\partial f_\alpha}{\partial v_z} = 0, \tag{16.112}$$

where $V_y(x,t) = -cE_0/B$ is the mean $\mathbf{E} \times \mathbf{B}$ drift of the plasma in the y-direction, $\delta\mathbf{E} = -\nabla\delta\phi$ and

$$\nabla^2 \delta\phi = -4\pi \sum_\alpha e_\alpha \int dv_z \delta\eta_\alpha. \tag{16.113}$$

We solve eqn (16.112) using a Laplace transform in time and Fourier transforms in z and y. Also, we assume that the fluctuations evolve rapidly in time compared to the slow time variation of f_α so that we may assume f_α and V_y are time-independent in eqn (16.112). Therefore in what follows we take $f_\alpha = f_\alpha(x, v_z)$ and $V_y = V_y(x)$. The solution to eqn (16.112) is then

$$\delta\eta_\alpha(\mathbf{r}, v_z, t) = \int_c \frac{dp}{2\pi i} e^{pt} \int \frac{dk_y dk_z}{(2\pi)^2} e^{ik_y y + ik_z z} \delta\hat{\eta}_\alpha(x, k_y, k_z, v_z, p) \tag{16.114}$$

where $\delta\hat{\eta}_\alpha$ satisfies

$$(p + ik_z v_z + ik_y V_y)\delta\hat{\eta}_\alpha = \left(ik_y \frac{c}{B} \frac{\partial f_\alpha}{\partial x} + ik_z \frac{e_\alpha}{m_\alpha} \frac{\partial f_\alpha}{\partial v_z} \right) \delta\hat{\phi} + \delta\hat{\eta}_{\alpha_0} \tag{16.115}$$

when $\delta\hat{\phi}(x, k_y, k_z, p)$ is the Fourier-Laplace transform of $\delta\phi$, and $\delta\hat{\eta}_{\alpha_0}(x, k_y, k_z, v_z)$ is the Fourier transform of the initial condition for $\delta\eta_\alpha$, $\delta\eta_{\alpha_0}(\mathbf{r}, v_z)$.

Exercise 16.11 Show that, if one assumes particles are *uncorrelated*,

$$\langle \delta\eta_{\alpha_0}(\mathbf{r}, v_z)\delta\eta_{\beta_0}(\mathbf{r}', v_z')\rangle = f_\alpha(x, v_z)\delta_{\alpha\beta}\delta(\mathbf{r}-\mathbf{r}')\delta(v_z - v_z') \tag{16.116}$$

and

$$\langle \delta\hat{\eta}_{\alpha_0}(x, k_y, k_z, v_z)\delta\hat{\eta}_{\beta_0}(x', k_y', k_z', v_z')\rangle = f_\alpha(x, v_z)\delta_{\alpha\beta}\delta(x-x')(2\pi)^2 \delta(k_y + k_y')\delta(k_z + k_z')\delta(v_z - v_z'). \tag{16.117}$$

Equation (16.115), when combined with Poisson's equation for the fluctuating potential $\delta\hat{\phi}$ yields the following expression for $\delta\hat{\phi}$:

$$\delta\hat{\phi}(x, k_y, k_z, p) = -4\pi \sum_\alpha e_\alpha \int dx' \psi(x, x', k_y, k_z, p) \int \frac{dv_z' \delta\hat{\eta}_{0_\alpha}(x', k_z, k_z, v_z')}{p + ik_z v_z' + ik_y V_y(x')} \tag{16.118}$$

where ψ is a Green's function for the potential, satisfying

$$\frac{\partial^2\psi}{\partial x^2} - \left[k_y^2 + k_z^2 - 4\pi i \sum_\alpha \frac{e_\alpha^2}{m_\alpha} \int dv_z \frac{\frac{k_y}{\Omega_\alpha}\frac{\partial f_\alpha}{\partial x} + k_z \frac{\partial f_\alpha}{\partial v_z}}{p + ik_z v_z + ik_y V_y}\right]\psi = \delta(x - x'), \tag{16.119}$$

and where $\Omega_\alpha = e_\alpha B/m_\alpha c$ is the cyclotron frequency for species α.

Equation (16.118) says that potential fluctuations at position x with wavenumbers (k_y, k_z) and frequency $\omega = ip$ are driven by discreteness in the particle distribution described by $\delta\hat{\eta}_{0\alpha}$, through the shielded Green's function ψ. Note that if $f_\alpha(x, v_z)$ were independent of x we could Fourier transform eqn (16.119) in x to obtain

$$\psi = -\int \frac{dk_x}{2\pi} \frac{e^{ik_x(x-x')}}{k^2 D_{\mathbf{k}p}} \tag{16.120}$$

where $D_{\mathbf{k}p}$ is a generalization of the plasma dielectric discussed in the previous section:

$$D_{\mathbf{k}p} = 1 - \frac{1}{k^2}\sum_\alpha \frac{4\pi i e_\alpha^2}{m_\alpha} k_z \int \frac{dv_z \partial f_\alpha/\partial v_z}{p + ik_z v_z + ik_y V_y}. \tag{16.121}$$

Comparing eqn (16.120) to eqn (16.89) reveals that ψ is a similar function to the function $\delta\phi$ discussed previously; it describes a Debye-shielded plasma response when $p + ik_y V_y \to 0$, and a wavelike response for $|\mathrm{Im}\, p| \gg k_z \bar{v}$.

In order to evaluate the collision operator, we require the two averages $\langle \delta E_y \delta\eta_\alpha\rangle$ and $\langle \delta E_z \delta\eta_\alpha\rangle$. (One can show by symmetry that $\langle \delta E_x \delta\eta_\alpha\rangle$ is zero.) These can be evaluated by first expressing δE_y (or δE_z) and $\delta\eta_\alpha$ in terms of their Fourier-Laplace transforms and then using eqn (16.115):

$$\langle \delta E_{\substack{y\\(z)}} \delta\eta_\alpha\rangle = -i\int \frac{dk_y' dk_z' dk_y dk_z}{(2\pi)^4} \int_c \frac{dp dp'}{(2\pi i)^2} e^{(p+p')t+i(k_y+k_y')y+i(k_z+k_z')z}$$
$$\times k'_{\substack{y\\(z)}} \left[i\frac{e_\alpha}{m_\alpha}\left(\frac{k_y}{\Omega_\alpha}\frac{\partial f_\alpha}{\partial x} + k_z\frac{\partial f_\alpha}{\partial v_z}\right)\langle \delta\hat\phi(x,k_y',k_z',p')\delta\hat\phi(x,k_y,k_z,p)\rangle \right.$$
$$\left. + \langle \delta\hat\phi(x,k_y',k_z',p')\delta\hat\eta_{0\alpha}(x,k_y,k_z,v_z)\rangle \right] / (p + ik_yV_y + ik_zv_z). \quad (16.122)$$

In turn, the two averages appearing in eqn (16.122) can be expressed in terms of the averages over initial fluctuations, given by eqn (16.117), by substituting eqn (16.118) for $\delta\hat\phi$:

$$\langle\ \delta\hat\phi(x,k_y',k_z',p')\delta\hat\eta_{0\alpha}(x,k_y,k_z,v_z)\rangle$$
$$= -4\pi\sum_\beta e_\beta \int dx' dv_z' \frac{\psi(x,x',k_y',k_z',p')}{p' + ik_z'v_z' + ik_y'V_y'}\langle\delta\hat\eta_{0\alpha}(x',k_y',k_z',v_z')\delta\hat\eta_{0\beta}(x,k_y,k_z,v_z)\rangle$$
$$= -4\pi e_\alpha \frac{\psi(x,x,-k_y,-k_z,p')}{p' - ik_zv_z - ik_yV_y}(2\pi)^2\delta(k_y+k_y')\delta(k_z+k_z')f_\alpha(x,v_z) \quad (16.123)$$

and

$$\langle\ \delta\hat\phi(x,k_y',k_z',p')\delta\hat\phi(x,k_y,k_z,p)\rangle$$
$$= (4\pi)^2\sum_\alpha\sum_\beta e_\alpha e_\beta \int dx' dv_z' dx'' dv_z'' \frac{\psi(x,x',k_y',k_z',p')\psi(x,x'',k_y,k_z,p)}{(p' + ik_z'v_z' + ik_y'V_y')(p + ik_zv_z'' + ik_yV_y'')}$$
$$\times\langle\delta\hat\eta_{0\alpha}(x',k_y',k_z',v_z')\delta\hat\eta_{0\beta}(x'',k_y,k_z,v_z'')\rangle$$
$$= (4\pi)^2\sum_\beta e_\beta^2 \int dx' dv_z' \frac{\psi(x,x',k_y',k_z',p')\psi(x,x',k_y,k_z,p)}{(p' + ik_zv_z' + ik_yV_y')(p + ik_zv_z' + ik_yV_y')}$$
$$\times(2\pi)^2\delta(k_y+k_y')\delta(k_z+k_z')f_\beta(x',v_z'), \quad (16.124)$$

where $V_y' \equiv V_y(x')$.

We must now perform the inverse Laplace transforms in eqn (16.122). In so doing note that poles in ψ are damped with $\mathrm{Re}\, p < 0$, so that at large times these poles do not contribute to the fluctuations. The only contributions that remain at large times arise from the resonant denominators, and lead to a time-independent result, just as in the case discussed in Sec. 4.1. It is useful to consider the contribution to eqn (16.122) of eqns (16.123) and (16.124) separately. Equation (16.123) contributes the term

$$-4\pi i\int \frac{dk_y dk_z}{(2\pi)^2} k_{\substack{y\\(z)}}\ e_\alpha\psi(x,x,-k_y,-k_z,i(k_yV_y+k_zv_z))f_\alpha(x,v_z) \quad (16.125)$$

and eqn (16.124) contributes the term

$$-(4\pi)^2\frac{e_\alpha}{m_\alpha}\sum_\beta e_\beta^2\int\frac{dk_y dk_z}{(2\pi)^2}\int dx'dv_z' k_{\substack{y\\(z)}}\ \left(\frac{k_y}{\Omega_\alpha}\frac{\partial f_\alpha}{\partial x}(x,v_z) + k_z\frac{\partial f_\alpha}{\partial v_z}(x,v_z)\right)$$
$$\times\ |\psi(x,x',+k_y,+k_z,-i(k_yV_y+k_zv_z))|^2 f_\beta(x',v_z')\pi\delta(k_y(V_y-V_y')+k_z(v_z-v_z')) \quad (16.126)$$

Here in evaluating the inverse Laplace transform we have used the identity

$$\lim_{t\to\infty} \mathrm{Re}\frac{e^{i(\omega'-\omega)t}-1}{i(\omega'-\omega)} = \pi\delta(\omega-\omega'). \tag{16.127}$$

(Only the real part contributes by symmetry of the integrand.) Also, we have used the identity

$$\psi(x,x',-k_y,-k_z,i\omega) = \psi^*(x,x',k_y,k_z,-i\omega) \tag{16.128}$$

which follows from eqn (16.119).

Expression (16.125) can be rewritten in a form that looks more like (16.126) by means of an identity that follows from eqn (16.119). Multiplying this equation by $\psi^*(x,k_y,k_z,-i\omega)$, integrating over x, and taking the imaginary part, yields

$$\begin{aligned}\mathrm{Im}\ \ \psi^*(x',x',k_y,k_z,-i\omega) = \mathrm{Im}\int dx\Bigg(&\psi^*(x,x',k_y,k_z,-i\omega)\frac{\partial^2\psi}{\partial x^2}(x,x',k_y,k_z,-i\omega)\\ -4\pi i\sum_\beta \frac{e_\beta^2}{m_\beta}\int dv_z &\frac{\frac{k_y}{\Omega_\beta}\frac{\partial f_\beta}{\partial x}+k_z\frac{\partial f_\beta}{\partial v_z}|\psi(x,x',k_y,k_z-i\omega)|^2}{ik_zv_z+ik_yV_y-i\omega+\varepsilon}\Bigg)\end{aligned} \tag{16.129}$$

where the infinitesimal ε in the denominator arises from the fact that the values of the Laplace transform variable $p=-i\omega$ must always lie to the right of poles. The first term in the integral over x vanishes because, on integration by parts, it has no imaginary part. Application of the Plemelj formula to second term allows one to extract the imaginary part analytically, yielding

$$\begin{aligned}\mathrm{Im}\psi^*(x',x',k_y,k_z,-i\omega) = -4\pi\sum_\beta\frac{e_\beta^2}{m_\beta}\int dxdv_z|\psi(x,x',k_y,k_z,-i\omega)|^2\\ \times\left(\frac{k_y}{\Omega_\beta}\frac{\partial f_\beta}{\partial x}+k_z\frac{\partial f_\beta}{\partial v_z}\right)\pi\delta(k_yv_z+k_yV_y-\omega).\end{aligned} \tag{16.130}$$

If we apply this identity to expression (16.125) and combine it with expression (16.126) we obtain the result

$$\begin{aligned}\langle\delta E_{\substack{y\\(z)}}\ \delta\eta_\alpha\rangle = e_\alpha\sum_\beta(4\pi e_\beta)^2\int\frac{dk_ydk_z}{(2\pi)^2}k_{\substack{y\\(z)}}\int dx'dv_z'\\ \times|\psi(x,x',k_y,k_z,-i(k_yV_y+k_zv_z))|^2\pi\delta(k_y(V_y-V_y')+k_z(v_z-v_z'))\\ \times\left[\frac{1}{m_\beta}\left(\frac{k_y}{\Omega_\beta}\frac{\partial f_\beta'}{\partial x'}+k_z\frac{\partial f_\beta'}{\partial v_z'}\right)f_\alpha-\frac{1}{m_\alpha}\left(\frac{k_y}{\Omega_\alpha}\frac{\partial f_\alpha}{\partial x}+k_z\frac{\partial f_\beta}{\partial v_z}\right)f_\beta'\right]\end{aligned} \tag{16.131}$$

where $f_\alpha = f_\alpha(x,v_z)$ and $f_\beta' = f_\beta(x',v_z')$. This result, along with eqn (16.111), provides the collision operator for long-range interactions in a magnetized plasma.

The operator describes shielded interactions between particles on different field lines at x and x'. The interaction is moderated by the Green's function ψ, which describes a Debye-shielded potential when the particles move slowly compared to $\bar{v}$, and

describes wave emission and absorption when they move rapidly. The δ function implies that the important interactions are resonant, so that a given Fourier component of the interaction provides a steady, time-independent force. The product of distribution functions in the square bracket is somewhat similar in form to the previous Boltzmann operator, eqn (16.66), representing the rate at which particles at (x, v_z) enter and leave the phase space element $dxdv_z$ due to collisions with particles at (x', v_z').

The collision operator satisfies several conservation laws. First, it clearly conserves particle number for each separate species, $\dot{N}_\alpha = \int dxdv_z \frac{\partial f_\alpha}{\partial t} = 0$. Second, total momentum along the field is conserved:

$$\dot{P}_z = \sum_\alpha \int dxdv_z m_\alpha v_z \frac{\partial f_\alpha}{\partial t} = -\sum_\alpha \int dxdv_z m_\alpha v_z C_\alpha[\mathbf{f}] = 0. \tag{16.132}$$

This follows by integration by parts of eqn (16.132), which yields

$$\begin{aligned}\dot{P}_z = \sum_{\alpha\beta}(4\pi e_\alpha e_\beta)^2 \int \frac{dk_y dk_z}{(2\pi)^2} k_z \int dxdv_z dx' dv_z' |\psi|^2 \\ \times \pi\delta(k_v(V_y - V_y') + k_z(v_z - v_z'))[...]\end{aligned} \tag{16.133}$$

where [...] stands for the square bracket in eqn (16.131). However, this bracket is antisymmetric under interchange of the dummy variables (x, v_z) and (x', v_z') and therefore the integral vanishes by symmetry, proving eqn (16.132). (Note that this requires $|\psi|^2$ to be symmetric on an interchange of x and x'. Proof of this is left as an exercise.)

Similar arguments imply that canonical momentum

$$P_y = \sum_\alpha \frac{e_\alpha B}{c} \int dxdv_z x f_\alpha \tag{16.134}$$

is conserved, as well as energy

$$E = \sum_\alpha \int dxdv_z \left(\frac{m_\alpha v_z^2}{2} + e_\alpha \phi_0\right) f_\alpha. \tag{16.135}$$

Exercise 16.12 Prove $\dot{P}_y = \dot{E} = 0$.

Finally, one can show that the collision operator maximizes the entropy functional $S[\mathbf{f}]$ where

$$S = -\sum_\alpha \int dxdv_z f_\alpha \ln f_\alpha. \tag{16.136}$$

Exercise 16.13 Show that $\dot{S} \geq 0$.

16.5 Heat Conduction, Viscosity and Diffusion due to Long-Range Collisions

In this lecture we will use the collision operator derived in the previous lecture to determine the cross-magnetic field heat conduction and viscosity of a plasma due to long-range collisions. We will also revisit the diffusion problem considered in Lecture 2.

16.5.1 Heat Conduction

As discussed in Lectures 1 and 3, the mechanism for heat conduction due to long-range collisions involves only motion parallel to the magnetic field $B\hat{z}$, and yields a result for the thermal conductivity that is essentially magnetic-field independent. Therefore in what follows we simplify the derivations by taking $B \to \infty$ so that we can neglect $\mathbf{E} \times \mathbf{B}$ drift corrections of $O(1/B)$. Also, we assume that there is only a single species. Furthermore, we assume that close velocity-scattering collisions not described by our collision operator keep the distribution function f a local Maxwellian with temperature $T(x,t)$:

$$f(x, v_z, v_\perp, t) = \frac{n}{(\sqrt{2\pi T(x,t)/m})^3} e^{-m(v_z^2+v_\perp^2)/2T(x,t)}. \tag{16.137}$$

Here we have explicitly kept the dependence of f on $v_\perp \equiv \sqrt{v_x^2 + v_y^2}$ because it will play a role in what follows. (We dropped this dependence in the previous two lectures because it was not needed.)

An evolution equation for the plasma temperature follows from the $B \to \infty$ version of eqn (16.110):

$$\frac{\partial f}{\partial t} = -\frac{e}{m}\frac{\partial}{\partial v_z}\langle \delta E_z \delta\eta \rangle. \tag{16.138}$$

This equation implies that plasma kinetic energy density, $K = \frac{3}{2}nT(x,t)$, evolves according to

$$\frac{3}{2}n\frac{\partial T}{\partial t} = \int d^3v \frac{m(v_z^2 + v_\perp^2)}{2}\frac{\partial f}{\partial t} = e\int dv_z v_z \langle \delta E_z \delta\eta \rangle. \tag{16.139}$$

The last expression is merely the Joule heating due to the parallel current fluctuations. This heats the parallel kinetic energy, but velocity-scattering collisions are assumed to be sufficiently rapid so that the energy is quickly shared with the perpendicular degrees of freedom, implying that the specific heat per particle is 3/2. This is why we kept perpendicular energy in f.

Using eqn (16.131) for $\langle \delta E_z \delta\eta \rangle$ and eqn (16.137) for f, we have

$$\frac{3}{2}n\frac{\partial T}{\partial t} = -\frac{e^2}{m}(4\pi e)^2 \int \frac{dk_y dk_z}{(2\pi)^2}\int d^3v d^3v' dx' k_z^2 v_z \times |\psi|^2(x, x', k_y, k_z, -ik_z v_z)\pi\delta(k_z(v_z - v_z'))ff'm\left(\frac{v_z'}{T(x')} - \frac{v_z}{T(x)}\right) \tag{16.140}$$

which implies

$$\frac{\partial T}{\partial t} = \frac{2}{3} m e^2 n (4\pi e)^2 \pi \int \frac{dk_z dk_z}{(2\pi)^2} \int dv_z dx' |k_z| v_z^2 \times |\psi|^2 \frac{(x, x', k_y, k_z, -ik_z v_2)}{2\pi \sqrt{T(x)T(x')}} e^{-m v_z^2 (1/T(x) + 1/T(x'))/2} \left(\frac{1}{T(x)} - \frac{1}{T(x')} \right) \quad (16.141)$$

This is very similar in form to eqn (16.68), obtained using the approximate Boltzmann formalism. Just as in that analysis, the integrand is odd under interchange of x and x'. If we (incorrectly) assume that the Green's function ψ is *local*, i.e. a sharply-peaked function of $x - x'$, we may obtain a local heat conduction equation using the same argument as in Lecture 3:

$$\frac{\partial T}{\partial t} = \frac{\partial}{\partial x} \chi \frac{\partial T}{\partial x} \quad (16.142)$$

where

$$\chi = \frac{2}{3} m e^2 n \frac{(4\pi e)^2 \pi}{T^3(x)} \int \frac{dk_y dk_z}{(2\pi)^3} \int dv_z dx' |k_z| v_z^2 e^{-m v_z^2 / T(x)} \times |\psi|^2 (x, x', k_y, k_z, -ik_z v_z) \frac{(x - x')^2}{2}. \quad (16.143)$$

Also, when $|\psi|^2$ is sharply peaked in $x - x'$, we can use the Fourier-transform form, eqn (16.120), for ψ, which implies that

$$\int |\psi|^2 \frac{(x - x')^2}{2} dx' = 2 \int \frac{dk_x}{2\pi} \frac{k_x^2}{k^8 |D_{\mathbf{k}, -ik_z v_z}|^4}, \quad (16.144)$$

where $D_{\mathbf{k}p}$ is given by eqn (16.88) [or eqn (16.93) with $v_0 = v_z$].

Exercise 16.14 Using eqn (16.120) prove eqn (16.144).

Then the local form of the thermal diffusivity due to long-range collisions is

$$\chi = \frac{2}{3} (4\pi e^2)^2 \frac{mn}{T^3} \int \frac{d^3 k}{(2\pi)^3} \int dv_z e^{-m v_z^2 / T} v_z^2 |k_z| k_x^2 / |k^2 D_{\mathbf{k}, -ik_z v_z}|^4. \quad (16.145)$$

If we approximate the dielectric function by a Debye-shielded form,

$$D_{\mathbf{k}, -ik_z v_z} = 1 + \frac{1}{k^2 \lambda_D^2}, \quad (16.146)$$

then the integrals can be performed, yielding

$$\chi^{\text{Debye}} = \frac{\sqrt{\pi}}{18} n \bar{v} b^2 \lambda_D^2 = \frac{e^2}{72\sqrt{\pi} m \bar{v}}. \quad (16.147)$$

However, we have seen in Lecture 4 that eqn (16.146) is correct only for $v_z = 0$. For $v_z > \bar{v}$, the dielectric exhibits near-zeros at $k_z v_z = \pm k_z \omega_p / k$, which cause the integrand in eqn (16.145) to blow up. This can be seen by using scaled variables $\bar{\mathbf{k}} = \mathbf{k} \lambda_D$ and

$\bar{v}_z = v_z/\bar{v}$ in eqn (16.145), and noting that D is a function only of $|\bar{\mathbf{k}}|$, $\bar{v}_z$ and the sign of $\bar{k}_z$ [see eqn (16.93)]. Then writing d^3k in spherical coordinates and integrating over solid angles yields

$$\chi = \frac{4}{3\pi} n\bar{v} b^2 \lambda_D^2 \int_0^\infty d\bar{k} g(\bar{k}) \tag{16.148}$$

where

$$g(\bar{k}) = \frac{\pi}{2}\bar{k}^5 \int_{-\infty}^{\infty} d\bar{v}_z \frac{\bar{v}_z^2 e^{-\bar{v}_z^2}}{[(\bar{k}^2 + a(\bar{v}_z))^2 + b^2(\bar{v}_z)]^2} \tag{16.149}$$

with the functions a and b given by eqn (16.94). Note that for small $\bar{k}$ there is a near zero in the denominator of the integrand where $\bar{k}^2 + a = 0$ and $|b| \ll 1$, due to weakly damped waves.

The function $g(\bar{k})$ is plotted in Fig. 16.10, and has a nonintegrable singularity at small $\bar{k}$. Our expression for thermal conduction diverges because weakly-damped waves are excited, and these waves transfer energy large distances across the plasma. This causes a breakdown in the local approximation used to obtain eqn (16.145) from eqn (16.141).

In order to obtain a non-divergent heat equation we must go beyond the local approximation. Returning to eqn (16.141), we instead assume only that $T(x)$ is nearly uniform,

$$T(x) = T + \delta T(x) \tag{16.150}$$

and we expand eqn (16.141) in small δT, obtaining

$$\begin{aligned}\frac{\partial T}{\partial t} = \frac{2}{3} m e^2 n \frac{(4\pi e)^2 \pi}{T^3} \int \frac{dk_y dk_z}{(2\pi)^3} \int dv_z dx' |k_z| v_z^2 e^{-mv_z^2/T} \\ \times |\psi|^2(x, x', k_y, k_z, -ik_z v_z)(\delta T(x') - \delta T(x)).\end{aligned} \tag{16.151}$$

Also, to lowest order in δT we can treat the plasma as a uniform slab of width L and we expand ψ in Fourier modes of the slab:

$$\psi(x, x', k_y, k_z, -ik_z v_z) = \frac{2}{L} \sum_{k_x} \frac{\sin(k_x x)\sin(k_x x')}{k^2 D_{\mathbf{k}, -ik_z v_z}} \tag{16.152}$$

where $k_x = n\pi/L$, $n = 1, 2, ...\infty$, and $k^2 = k_x^2 + k_y^2 + k_z^2$.

For large plasmas with $L \gg \lambda_D$, we evaluate the integrals in eqn (16.151) asymptotically in the small parameter $\varepsilon \equiv \pi\lambda_D/L$. Since $|\psi|^2$ appears in eqn (16.151), a double sum over k_x appears, as $\sum_{k_x}\sum_{k_x'}$. However the flux is dominated by $k_x \simeq k_x'$; otherwise the integral phase-mixes away upon integration over x' [because $\delta T(x)$ varies slowly but $\sin k_x x$ varies rapidly for k_x of $O(\lambda_D^{-1})$]. Writing $\sin(k_x x')\sin(k_x' x') = 1/2[\cos(k_x - k_x')x' - \cos(k_x + k_x')x']$ and dropping the second term because of phase-mixing, we obtain

$$\frac{\partial T}{\partial t} = \frac{2}{3} m e^2 n \frac{(4\pi e)^2 \pi}{T^3} \int \frac{dk_y dk_z}{(2\pi)^3} \int dv_z dx' \times |k_z| v_z^2 e^{-m v_z^2/T} \frac{1}{L^2} \sum_{k_x} \sum_{\Delta k_x} \frac{1}{k^2 D_{\mathbf{k},-ik_z v_z} k'^2 D^*_{\mathbf{k}',-ik_z v_z}} \times \cos(\Delta k_x x) \cos(\Delta k_x x')(\delta T(x') - \delta T(x)) \tag{16.153}$$

where $\Delta k_x = k'_x - k_x$.

As $\varepsilon \to 0$ the integrand takes two asymptotic forms, depending on the size of $k\lambda_D$. These forms can be asymptotically matched at $k\lambda_D = 0.4$. For $k\lambda_D > 0.4$, there are no lightly-damped waves and $1/D$ varies slowly in k. Then Taylor expanding $1/k'^2 D_{\mathbf{k}',-ik_z v_z}$ in Δk_x one finds that the $(\Delta k_x)^0$ term in eqn (16.153) vanishes because

$$\sum_{\Delta k_x} \cos \Delta k_x x \int_0^L dx' \cos \Delta k_x x' (T(x') - T(x)) = 0. \tag{16.154}$$

One may show this directly by writing $T(x)$ and $T(x')$ as Fourier cosine series, and performing the integral in eqn (16.154). Also the $(\Delta k_x)^1$ term in eqn (16.153) vanishes because it is odd in Δk_x, and the $O(\Delta k_x^2)$ term leads back to the local form for the heat equation with χ given by eqn (16.145), except that the integral over k in χ is limited to $k\lambda_D > 0.4$.

For $k\lambda_D < 0.4$, lightly-damped waves provide the main contribution to the integral. When v_z approaches a zero of the dielectric function, $1/D_{\mathbf{k},-ik_z v_z} D^*_{\mathbf{k}',-ik_z v_z}$ becomes sharply peaked at the points $v_z = v_0$ and $v_z = v'_0$, where v_0 and v'_0 satisfy

$$k^2 \lambda_D^2 + a(v_0/\bar{v}) = 0 \tag{16.155}$$

and

$$k'^2 \lambda_D^2 + a(v'_0/\bar{v}) = 0; \tag{16.156}$$

see eqn (16.93). Note that for $k\lambda_D \ll 1$ each equation has two solutions, since a is an even function and $a < 0$. When $k\lambda_D \ll 1$, v_0 is such that $b(v_0/\bar{v}) \ll 1$, and similarly for $b' \equiv b(v'_0/\bar{v})$. Then upon integrating over the sharp peaks we obtain

$$\int_{k^2 k'^2} \frac{dv_z}{D_{\mathbf{k}-ik_z v_z} D^*_{\mathbf{k}-ik_z v_z}} \simeq \int \frac{dv_z \lambda_D^4}{[\frac{\partial a}{\partial v_0}(v_z - v_0) + ib\, sgn(k_z)][\frac{\partial a}{\partial v'_0}(v_z - v'_0) - ib'\, sgn(k_z)]} = \frac{2\pi \lambda_D^4}{\frac{\partial a}{\partial v_0}\frac{\partial a}{\partial v'_0}} \frac{\bar{\gamma} - i\Delta v\, sgn(k_z)}{\bar{\gamma}^2 + \Delta v^2} \tag{16.157}$$

where $\bar{\gamma} = b/\partial a/\partial v_0 + b'/\partial a/\partial v'_0$ and $\Delta v = v_0 - v'_0$. [This result must be doubled to account for the second negative solution of eqns (16.155) and (16.156).] Substituting this expression into eqn (16.153), the imaginary part vanishes because it is odd both in k_z and under interchange of k_x and k'_x. Also, we note that one can add to the rhs of eqn (16.157) any function that is independent of Δk_x [this follows from eqn (16.154)]. We therefore subtract $\pi \lambda_D^4/(b\, \partial a/\partial v_0)$, which causes the integrand to vanish at $\Delta k_x =$

0. Turning the sum over $k_x \geq 0$ into an integral over all k_x, dividing by two and multiplying by two because eqn (16.155) has two roots for v_0, yields

$$\frac{\partial T^{\rm waves}}{\partial t} = \frac{2}{3} m e^2 n \frac{(4\pi e)^2 \pi}{T^3} \lambda_D^4 \int\limits_{k\lambda_D > 0.4} \frac{d^3k}{(2\pi)^3} \int dx' |k_z| v_0^2 e^{-mv_0/T} \times \frac{1}{\pi L} \sum_{\Delta k_x} \left(\frac{2\pi}{\frac{\partial a}{\partial v_0}\frac{\partial a}{\partial v_0'}} \frac{\bar{\gamma}}{\bar{\gamma}^2 + \Delta v^2} - \frac{\pi}{b\frac{\partial a}{\partial v_0}} \right) \times \cos \Delta k_x x \, \cos \Delta k_x x' (\delta T(x') - \delta T(x)). \tag{16.158}$$

The main contribution arises from $\Delta k_x \ll k_x$, allowing us to take $\partial a/\partial v_0 \simeq \partial a/\partial v_0'$, and $\bar{\gamma} \simeq 2b \, sgn(k_z)/(\partial a/\partial v_0)$. This also implies $\Delta v = -2k_x \Delta k_x/(\partial a/\partial v_0)$ [see eqns (16.155) and (16.156)].

If we now integrate by parts in x' and define $\Delta k_x = j\pi/L$, we can write eqn (16.158) as

$$\frac{\partial T^{\rm waves}}{\partial t} = \frac{2}{3} m e^2 n \frac{(4\pi e)^2 \pi \lambda_D^4}{T^3} \int\limits_{k\lambda_D < 0.4} \frac{d^3k}{(2\pi)^3} |k_z| v_0^2 e^{-mv_0^2/T} \times \sum_{j=1}^{\infty} \hat{T}_j \frac{\partial}{\partial x} (\sin \Delta k_x x) \frac{\partial a/\partial v_0}{b} \frac{\Delta v^2/\Delta k_x^2}{4b^2 + \Delta v^2 (\partial a/\partial v_0)^2} \tag{16.159}$$

where $\hat{T}_j \equiv 2/L \int dx' \, \sin(j\pi x'/L) \, \partial T/\partial x'$ is the Fourier coefficient of the temperature gradient. Finally, we add to eqn (16.159) the contribution from $k\lambda_D > 0.4$ to obtain the total rate of change of T (Dubin and O'Neil 1997):

$$\frac{\partial T}{\partial t} = \frac{\partial}{\partial x} \sum_{j=1}^{\infty} (\chi^{\rm local} + \chi_j^{\rm waves}) \hat{T}_j \, \sin \frac{j\pi x}{L}. \tag{16.160}$$

Here,

$$\chi^{\rm local} = \frac{4}{3\pi} n \bar{v} b^2 \lambda_D^2 \int\limits_{0.4}^{\infty} d\bar{k} g(\bar{k}), \tag{16.161}$$

is the local contribution to the thermal diffusivity, with g given by eqn (16.149). Also,

$$\chi_j^{\rm waves} = \frac{4}{3\pi} n \bar{v} b^2 \lambda_D^2 \int\limits_{0}^{0.4} d\bar{k} h(\bar{k}, j\varepsilon) \tag{16.162}$$

is the wave contribution to the thermal diffusivity, where

$$h(\bar{k}, \varepsilon) = \pi \int d\Omega \bar{k}^2 |\bar{k}_z| \frac{\bar{v}_0^2 e^{-\bar{v}_0^2}}{\frac{\partial a}{\partial \bar{v}_0} b(\bar{v}_0)} \frac{\bar{k}_x^2}{b^2(\bar{v}_0) + \bar{k}_x^2 j^2 \varepsilon^2}, \tag{16.163}$$

$\bar{v}_0 = v_0/\bar{v}$, and $d\Omega$ is the element of solid angle that arises in $d^3\bar{k} = \bar{k}^2 d\bar{k} d\Omega$. When evaluating eqn (16.163), recall that $\bar{v}_0$ is a function of $k\lambda_D$ through the solution of eqn (16.155); it is the (scaled) phase velocity of weakly-damped plasma waves.

Table 16.2 Wave contribution to heat flux

$j\varepsilon$	$\chi^j_{\rm waves}/(e^2/m\bar{v})$
0.1	0.0115
0.05	0.0262
0.01	0.102
0.005	0.167
0.001	0.518
0.0005	0.859
10^{-4}	2.93
10^{-5}	19.0

The functions $g(\bar{k})$ and $h(\bar{k}, j\varepsilon)$ are plotted in Fig. 16.10. For $j\varepsilon \ll 1$, they can be matched at $\bar{k} \sim 0.4$. Note that h is not divergent at small $\bar{k}$ so the heat flux is now finite, depending on the scale length $L_j = L/j\pi$ of the temperature gradient through the parameter $j\varepsilon$.

A numerical integration yields

$$\chi^{\rm local} = 0.0652 e^2/m\bar{v} = 0.819\nu_0\lambda_D^2. \tag{16.164}$$

Equation (16.164) is an order of magnitude larger than the value obtained from simple Debye shielding, eqn (16.147). This is because the interaction cannot be accurately characterized by the simple Debye-shielding dielectric response, even when $k\lambda_D > 0.4$. Off-resonant plasma waves greatly increase $g(\bar{k})$ compared to the form $g(\bar{k})$ would take using simple Debye shielding, $g^{\rm Debye}(\bar{k})$ obtained by setting $a = 1$ and $b = 0$ in eqn (16.149),

$$g^{\rm Debye}(\bar{k}) = \frac{\pi^{3/2}}{4}\frac{\bar{k}^5}{(1+\bar{k}^2)^4}. \tag{16.165}$$

Only for $\bar{k} \gtrsim 3$ do the functions approach one another–see Fig. 16.10.

Values for $\chi_j^{\rm waves}$ are provided in Table 16.5.1. These values differ slightly from those in Dubin and O'Neil (1997), because here we use a more accurate solution to eqn (16.155) in determining the function $h(j\varepsilon, \bar{k})$. Table I of Dubin and O'Neil (1997) provides values of $\kappa^j_{\rm waves} = 3/2\, n\kappa^j_{\rm waves}$. Some other references [e.g. Dubin (1998) and Hollman *et al.* (2000)] quote a different value of χ based on a "neutral plasma" heat capacity of 5/2 rather than 3/2 (i.e. the heat capacity at constant pressure rather than at constant volume). The resulting factor of 3/5 must be accounted for when comparing formulas for χ in those papers with those quoted here.

The table shows that when the scale length of the temperature gradient L_j is greater than about $100\lambda_D$, emission and absorption of lightly damped waves is the dominant heat transport mechanism. For L_j less than this, a local theory of thermal conduction suffices, with $\chi^{\rm local}$ given by eqn (16.164).

Experiments have tested the theory in the regime where $\lambda_D > \bar{r}_c$ and $L_j < 100\lambda_D$, where the transport is local (Hollmann *et al.* 2000). In the experiments, the laser-diagnosed Mg^+ plasma described in Lecture 2 is again used. Now the lasers are used both to manipulate the initial plasma temperature, and to diagnose the resulting

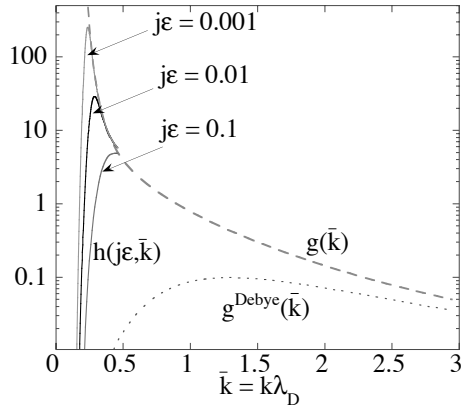

Fig. 16.10 The functions $g(\bar{k})$, $g^{\mathrm{Debye}}(\bar{k})$ and $h(j\varepsilon, \bar{k})$ for three values of $j\varepsilon$.

temperature evolution. First, the plasma is brought to a near-uniform temperature with a slight peak at $r = 0$. Then the laser is turned off, and the evolution of $T(r, t)$ is recorded. Using the same basic methodology for measuring test particle transport, the temperature data is compared to the prediction of Fourier's Law, that radial heat flux is proportional to the local temperature gradient. The coefficient of proportionality is the local thermal diffusivity χ^{local}. Results of several such measurements are shown in Fig. 16.11 and compared to both eqn (16.164) and the classical theory (Table 16.1), versus temperature. Here n_7 is density in units of $10^7\,\mathrm{cm}^{-3}$, and B is in Tesla. The results are independent of magnetic field and density, as predicted by eqn (16.164), and are in quantitative agreement with the theory within a factor of 2.

16.5.2 Viscosity

We now consider viscous relaxation due to long-range collisions in a plasma for which there is a shear flow with $\mathbf{V} = V_y(x)\hat{y}$. For simplicity we assume a single species with uniform density and temperature. The distribution function is then

$$f(v_z) = \frac{ne^{-mv_z^2/2T}}{\sqrt{2\pi T/m}}. \tag{16.166}$$

Viscous relaxation in such a plasma manifests itself through a cross field particle flux Γ_x. This flux arises because the shear flow creates a shear stress in the y-direction (i.e. a force density):

$$F_y = \frac{\partial}{\partial x}\eta\frac{\partial V_y}{\partial x} \tag{16.167}$$

[see eqn (16.20)]. In a magnetized plasma this force density creates an $\mathbf{F} \times \mathbf{B}$ drift (the equivalent to an $\mathbf{E} \times \mathbf{B}$ drift except for a general force rather than an electric field):

$$\Gamma_x = \frac{c}{eB}F_y = \frac{c}{eB}\frac{\partial}{\partial x}\eta\frac{\partial V_y}{\partial x}. \tag{16.168}$$

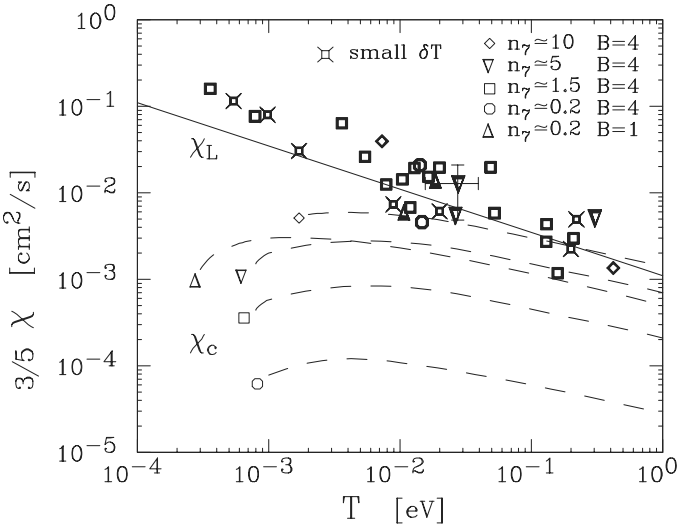

Fig. 16.11 Comparison of experimentally-measured thermal diffusivity to theory. Solid line is eqn (16.164), dashed lines are classical theory at different densities and magnetic fields used in the experiment. The factor of 3/5 arises due to a different definition of χ used in Hollmann *et al.* (2000).

Using eqns (16.110), (16.111) and (16.131) we can obtain the following expression for the particle flux due to long-range collisions, which should be equivalent to eqn (16.168):

$$\begin{aligned}\Gamma_x &= \int dv_z \frac{c}{B}\langle \delta E_y \delta\eta\rangle \\ &= \frac{ec}{mB}(4\pi e)^2 \int dx' dv_z' dv_z \int \frac{dk_y dk_z}{(2\pi)^2} k_y \pi \delta(k_z(v_z - v_z') + k_y(V_y - V_y')) \\ &\quad \times |\psi|^2(x, x', k_y, k_z, -ik_y V_y - ik_z v_z) \frac{m^2 n^2}{2\pi T^2} k_z (v_z - v_z') e^{-m/2T(v_z^2 + v_z'^2)} \end{aligned} \quad (16.169)$$

Using the δ-function, we may replace the $k_z(v_z - v_z')$ term in the integrand by $k_y(V_y' - V_y)$. Hence, the flux is proportional to a difference in the fluid velocity at points x and x'.

If $|\psi|^2$ is *assumed* to be a sharply peaked function of $x - x'$, a local approximation to the flux can be made, just as was done previously for heat transport. We then obtain, in a manner entirely analogous to the derivation of the local form of heat conduction,

$$\Gamma_x = \frac{c}{eB}\frac{\partial}{\partial x}\left(mn\lambda \frac{\partial V_y}{\partial x}\right) \quad (16.170)$$

with the kinematic viscosity λ given by

$$\lambda = \frac{(4\pi e^2)^2 n}{T^2} \int dv_z e^{-mv_z^2/T} \int \frac{d^3k}{(2\pi)^3} \frac{k_x^2 k_y^2}{|k_z||k^2 D_{\mathbf{k}, -ik_z v_z}|^4}. \quad (16.171)$$

Here we have simplified the expression for λ by assuming B is large so that we can neglect $k_y V_y$ compared to $k_z v_z$. This expression for the local kinematic viscosity due to long range collisions can be easily evaluated if one assumes a Debye-shielded response, $D = 1 + 1/k^2\lambda_D^2$. Noting the logarithmic divergence at small k_z must be cut off at $k_{z\,\min} = \mathrm{Max}(S,\nu)/\bar{v}$ in order to properly account for velocity diffusion (and include the factor of 3 enhancement effect due to collisional caging discussed in Lecture 2), we can write eqn (16.171) to logarithmic order as (O'Neil 1985)

$$\lambda = \frac{(4\pi e^2)^2 n}{T^2}\sqrt{\pi}\bar{v}\int \frac{dk_\perp k_\perp d\theta}{(2\pi)^3}\frac{k_\perp^4 \sin^2\theta\cos^2\theta}{(k_\perp^2+\lambda_D^{-2})^4} 2\int_{k_{z_{\min}}}^{\lambda_D^{-1}} \frac{dk_z}{|k_z|}$$

$$= \frac{\sqrt{\pi}}{6} n\bar{v}b^2\lambda_D^2 \ln\left(\frac{\omega_p}{\mathrm{Max}(S,\nu)}\right). \tag{16.172}$$

However, if we use the full dielectric response we again find a nonlocal contribution due to lightly-damped waves that cannot be neglected. A calculation analogous to that given previously for thermal conduction yields

$$\Gamma_x = \frac{n}{\Omega_c}\frac{\partial}{\partial x}\sum_{j=1}^{\infty}(\lambda^{\mathrm{local}} + \lambda_j^{\mathrm{waves}})\,\hat{V}_j \frac{\sin j\pi x}{L} \tag{16.173}$$

where $\hat{V}_j$ is the jth Fourier coefficient of $\partial V_y/\partial x$,

$$\hat{V}_j = \frac{2}{L}\int_0^L dx \frac{\partial V_y}{\partial x}\frac{\sin j\pi x}{L}. \tag{16.174}$$

Here λ^{local} is the local contribution due to wave numbers $k\lambda_D > 0.4$, given by

$$\lambda^{\mathrm{local}} = 0.0465\frac{e^2}{m\bar{v}}\ln\left(\frac{\omega_p}{\mathrm{Max}(S,\nu)}\right) = 0.585\nu_0\lambda_D^2\ln\left(\frac{\omega_p}{\mathrm{Max}(S,\nu)}\right), \tag{16.175}$$

roughly twice the result given by simple Debye shielding, eqn (16.172). The wave contribution is

$$\lambda_j^{\mathrm{waves}} = n\bar{v}b^2\lambda_D^2\ln\left(\frac{\omega_p}{\mathrm{Max}(S,\nu)}\right)\int_0^{0.4} d\bar{k}_\perp h_\lambda(\bar{k}_\perp, j\varepsilon) \tag{16.176}$$

with

$$h_\lambda = \frac{4\bar{k}_\perp^5 e^{-\bar{v}_0^2}}{\frac{\partial a}{\partial \bar{v}_0}b(\bar{v}_0)}\int_0^{2\pi} d\theta \frac{\cos^2\theta\sin^2\theta}{b^2(\bar{v}_0) + (\bar{k}_\perp j\varepsilon)^2\cos^2\theta}, \tag{16.177}$$

where the functions a and b are given by eqn (16.94), $\bar{v}_0 = v_0/\bar{v}$ is the solution to eqn (16.155) taking $k_z = 0$, and $\bar{k}_\perp = k_\perp\lambda_D$.

Table 16.3 Wave contribution to viscosity

$j\varepsilon$	$\lambda_j^{\text{waves}}\ (\ln(\omega_p/\text{Max}(S,\nu))e^2/m\bar{v})$
0.1	1.45×10^{-3}
0.05	3.19×10^{-3}
0.01	1.06×10^{-2}
0.005	1.61×10^{-2}
0.001	4.11×10^{-2}
0.0005	6.29×10^{-2}
10^{-4}	0.181
10^{-5}	0.955

Table 16.4 Transport coefficients due to long-range collisions in a single species plasma with $\lambda_D > \bar{r}_c$. In this regime these coefficients must be added to the classical results (Table 16.1).

D	χ	λ
$2\sqrt{\pi}\nu_0\bar{r}_c^2\ln(\frac{\lambda_D}{\bar{r}_c})\ln(\frac{\bar{v}}{\gamma\sqrt{\lambda_D\bar{r}_c}})$	$0.0652\,e^2/m\bar{v}$ + wave contribution important for $L_j > 100\,\lambda_D$	$0.0465(e^2/m\bar{v})\ \ln(\frac{\omega_p}{\gamma})$ + wave contribution important for $L_j > 10^3\lambda_D$
$S \equiv \lvert\partial V_y/\partial x\rvert\ ,\ \ \nu_0 \equiv n\bar{v}b^2,$	$\gamma \equiv \text{Max}(S,\nu)$	

The wave contribution is tabulated in Table 16.5.2. One can see that waves are important to viscous transport only when the scale length of the shear flow $L_j = L/j\pi$ exceeds roughly 1000 Debye lengths.

The wave contribution to viscosity is an order of magnitude smaller than the corresponding contribution to thermal conduction. Evidently weakly damped plasma waves transmit energy more efficiently than momentum. So far there have been no experiments to test these results in detail. However, some experiments have been performed that measured viscosities consistent with eqn (16.175) (Kriesel and Driscoll 2001). More experiments need to be done to test the density, temperature and magnetic field dependence of the viscosity coefficient.

Table 5.3 summarizes our results for the flux of particles, energy and momentum caused by long range collisions.

16.5.3 Diffusion Revisited, and the Ludwig-Soret Effect

As a final application of the new collision operator, we reanalyze particle diffusion due to long range collisions where there are several species and temperature gradients. We also consider the effects of lightly damped waves on diffusion. We will find that such effects are negligible, justifying our neglecting them in Lecture 2. By including temperature gradients, we will predict a new transport coefficient related to the Ludwig-Soret effect, wherein a temperature gradient induces a particle flux in a multi-species system.

The system is assumed to be at temperature $T(x)$, and as always velocity-scattering collisions keep the distribution function for each species in a local Maxwellian form,

$$f_\alpha(x,v_z)=\frac{n_\alpha(x)}{\sqrt{2\pi T(x)/m_\alpha}}e^{-m_\alpha v_z^2/2T(x)}. \tag{16.178}$$

Equation (16.131) then implies the following expression for the particle flux of species α:

$$\begin{aligned}\Gamma_{\alpha_x}(x)&=\int dv_z\frac{c}{B}\langle\delta E_y\delta\eta_\alpha\rangle\\
&=\frac{ce_\alpha}{B}\sum_\beta(4\pi e_\beta)^2\int dx'dv_z'dv_z\int\frac{dk_ydk_z}{(2\pi)^2}k_y|\psi|^2(x,x',k_y,k_z,-ik_yV_y-ik_zv_z)\\
&\quad\times\pi\delta(k_z(v_z-v_z')+k_y(V_y-V_y'))\frac{\sqrt{m_\alpha m_\beta}}{2\pi\sqrt{TT'}}e^{-\left(\frac{m_\alpha v_z^2}{2T}+\frac{m_\beta v_z'^2}{2T'}\right)}\\
&\quad\left\{\frac{n_\alpha}{m_\beta}\left(\frac{k_y}{\Omega_{c_\beta}}\left[\frac{\partial n_\beta'}{\partial x'}+\frac{n_\beta'}{T'}\frac{\partial T'}{\partial x'}\left(\frac{m_\beta v_z'^2}{2T'}-\frac{1}{2}\right)\right]-\frac{m_\beta v_z'}{T'}k_zn_\beta'\right)\right.\\
&\quad\left.-\frac{n_\beta'}{m_\alpha}\left(\frac{k_y}{\Omega_{c_\alpha}}\left[\frac{\partial n_\alpha}{\partial x}+\frac{n_\alpha}{T}\frac{\partial T}{\partial x}\left(\frac{m_\alpha v_z^2}{2T}-\frac{1}{2}\right)\right]-\frac{m_\alpha v_z}{T}k_zn_\alpha\right)\right\}.\end{aligned} \tag{16.179}$$

We assume that $|\psi|^2$ is strongly peaked in $x-x'$, so that everywhere in the integrand except in $|\psi|^2$ itself we may take $x'=x$. The δ function then implies $v_z=v_z'$, and eqn (16.179) becomes

$$\Gamma_{\alpha_x}=-\sum_\beta\left(D_{\alpha\beta}\frac{\partial n_\alpha}{\partial x}-\bar D_{\alpha\beta}\frac{\partial n_\beta}{\partial x}\right)+\gamma_\alpha\frac{\partial T}{\partial x} \tag{16.180}$$

where

$$D_{\alpha\beta}=\left(\frac{4\pi e_\beta c}{B}\right)^2\frac{n_\beta}{2T}\sqrt{m_\alpha m_\beta}\int\frac{dk_ydk_z}{(2\pi)^2}\frac{k_y^2}{|k_z|}\int dx'dv_z|\psi|^2e^{-(m_\alpha+m_\beta)v_z^2/2T} \tag{16.181}$$

is the diffusion coefficient of species α due to collisions with species β and $\bar D_{\alpha\beta}$ is an "off-diagonal" diffusion coefficient, producing a flux of species α due to gradients in other species. The diffusion coefficient $\bar D_{\alpha\beta}$ is related to $D_{\alpha\beta}$ via

$$e_\beta n_\beta\bar D_{\alpha\beta}=e_\alpha n_\alpha D_{\alpha\beta}. \tag{16.182}$$

Note that when there is only a single species, eqns (16.180) and (16.182) imply that the diffusive flux vanishes, as expected. For a single species the flux is viscous, not diffusive. When there are two species with identical mass and charge that have some other property that discriminates them, such as their spin, eqn (16.180) and (16.182) are equivalent to eqn (16.42) for the flux of test particles through a background plasma of like particles.

The Ludwig-Soret coefficient γ_α provides the particle flux of species α due to a temperature gradient:

$$\begin{aligned}\gamma_\alpha&=\frac{ce_\alpha}{2B}\sum_\beta(4\pi e_\beta)^2n_\alpha n_\beta\int dx'dv_z\int\frac{dk_ydk_z}{(2\pi)^2}\frac{k_y^2}{|k_z|}|\psi|^2\frac{\sqrt{m_\alpha m_\beta}}{T^2}e^{-\frac{(m_\alpha+m_\beta)}{2T}v_z^2}\\
&\quad\times\left[\frac{1}{m_\beta\Omega_{c_\beta}}\left(\frac{m_\beta v_z^2}{2T}-\frac{1}{2}\right)-\frac{1}{m_\alpha\Omega_{c_\alpha}}\left(\frac{m_\alpha v_z^2}{2T}-\frac{1}{2}\right)\right].\end{aligned} \tag{16.183}$$

The above expressions for $D_{\alpha\beta}$ and γ_α are evaluated under the assumption that $|\psi|^2$ is sharply peaked. Spatial variation in the coefficients of eqn (16.119) can then be neglected, from which Parseval's theorem implies

$$\int dx' |\psi|^2 = \int \frac{dk_x}{2\pi} \frac{1}{|k^2 D_{\mathbf{k},-ik_z v_z}|^2}. \tag{16.184}$$

Thus, eqn (16.181) may be written as

$$D_{\alpha\beta} = \left(\frac{4\pi e_\beta c}{B}\right)^2 \frac{n_\beta}{2T}\sqrt{m_\alpha m_\beta} \int \frac{d^3k dv_z}{(2\pi)^3} \frac{k_y^2}{|k_z||k^2 D_{\mathbf{k},-ik_z v_z}|^2} e^{-(m_\alpha+m_\beta)v_z^2/2T}. \tag{16.185}$$

Noting the log divergence at small k_z and cutting it off in the usual manner at $k_{z\,\min} = \mathrm{Max}(S,\nu)/\bar{v}$ and $k_{z\,\max} = k_\perp$, eqn (16.185) becomes

$$D_{\alpha\beta} = \left(\frac{4\pi e_\beta c}{B}\right)^2 \frac{n_\beta}{T}\sqrt{m_\alpha m_\beta} \int \frac{dv_z d\bar{k}_\perp}{(2\pi)^3} \frac{\pi \bar{k}_\perp^3 e^{-(m_\alpha+m_\beta)v_z^2/2T}}{(\bar{k}_\perp^2 + a(v_z/\bar{v}))^2 + b^2(v_z/\bar{v}))} \log\left(\frac{\bar{k}_\perp \omega_p}{\mathrm{Max}(S,\nu)}\right), \tag{16.186}$$

where $\bar{k}_\perp \equiv k_\perp \lambda_D$. While the denominator does exhibit near zeros due to lightly damped waves, these occur only for $\bar{k}_\perp < 1$. However, the integrand is dominated by the logarithmic divergence at large $\bar{k}_\perp$, which we cut off at $\bar{k}_\perp \simeq \lambda_D/\bar{r}_c$, where here $\bar{r}_c$ is the mean cyclotron radius for species α and β.

In this range of $\bar{k}_\perp$ the integrand can be approximated by neglecting a and b (i.e. using unshielded interactions), yielding

$$\begin{aligned} D_{\alpha\beta} &= \left(\frac{4\pi e_\beta c}{B}\right)^2 \frac{n_\beta}{T}\sqrt{m_\alpha m_\beta}\frac{\pi}{(2\pi)^3} \int dv_z e^{-(m_\alpha+m_\beta)/v_z^2 2T} \int_1^{\lambda_D/\bar{r}_c} \frac{d\bar{k}_\perp}{\bar{k}_\perp} \ln\left(\frac{\bar{k}_\perp \omega_p}{\nu}\right) \\ &= 2\sqrt{\pi}\left(\frac{e_\beta c}{B}\right)^2 n_\beta \sqrt{\frac{2m_\alpha m_\beta}{(m_\alpha+m_\beta)T}} \ln\left(\frac{\lambda_D}{\bar{r}_c}\right) \ln\left(\frac{\bar{v}}{\mathrm{Max}(S,\nu)\sqrt{\lambda_D \bar{r}_c}}\right). \end{aligned} \tag{16.187}$$

Thus, lightly-damped waves have a negligible effect on the diffusion coefficient, justifying the analysis of Lecture 2. For a single species, eqn (16.187) is the same as eqn (16.59).

Applying the same analysis to the Ludwig-Soret coefficient, eqn (16.183), yields

$$\gamma_\alpha = \sum_\beta \frac{n_\alpha m_\beta D_{\alpha\beta} - n_\beta m_\alpha \bar{D}_{\alpha\beta}}{2T(m_\alpha+m_\beta)}. \tag{16.188}$$

As expected, this coefficient vanishes in a single species system.

16.6 Enhanced Transport in Nearly 2D Plasmas

The theory of transport due to long range collisions, summarized in Table 16.5.2, assumes plasmas of infinite extent along the magnetic field direction $\hat{z}$. However, new effects come into play for plasmas that are of finite length L_z when both the collision

frequency ν and shear rate S are small compared to the frequency $\omega_B = \pi\bar{v}/L_z$ at which particles bounce from end to end of the plasma. When this axial bounce frequency is large, particles encounter one another many times as they bounce, just as in the collisional caging phenomenon discussed in Lecture 2, except that now the ends of the plasma (rather than surrounding particles) act to cage the particles. The effect of these multiple encounters is to increase the correlation time of the interactions, leading to larger particle diffusion and viscosity (we will see that thermal diffusion is largely unaffected).

This effect is already contained in our collision operator. Let us apply it to a system of finite length with *periodic* boundary conditions in z of length L_z; the argument can be generalized to more realistic boundary conditions (Dubin and O'Neil 1998). Imposition of periodic boundary conditions has the effect of replacing the integral over k_z in eqn (16.179) by a sum, $\int dk_z \to \frac{2\pi}{L_z}\sum_{k_z}$. This sum includes a $k_z = 0$ term, representing the z-averaged (or "bounce-averaged") interaction. In our previous derivations this term did not enter. The contribution of $k_z = 0$ to the flux is

$$\Gamma_\alpha^{k_z=0} = \frac{ce_\alpha}{B}\sum_\beta (4\pi e_\beta)^2 \int dx' \frac{dk_y}{2\pi L_z} k_y^2 |\psi|^2(x, x', k_y, 0, -ik_y V_y) \times \pi\delta(k_y(V_y - V_y')) \left[\frac{n_\alpha}{m_\beta \Omega_{c_\beta}}\frac{\partial n_\beta'}{\partial x'} - \frac{n_\beta'}{m_\alpha \Omega_{c_\alpha}}\frac{\partial n_\alpha}{\partial x}\right], \tag{16.189}$$

where we have dropped temperature gradients for simplicity.

If $V_y(x)$ is not a monotonic function of x, the δ function allows resonant interactions between separate x and x' points that obey $V_y = V_y'$, leading to enhanced viscosity (Dubin and O'Neil 1988). However, if $V_y(x)$ is monotonic only $x = x'$ satisfies $V_y = V_y'$ and eqn (16.189) predicts a diffusive contribution to the flux with a diffusion coefficient $D_{\alpha\beta}^{2D}$ given by

$$D_{\alpha\beta}^{2D} = \sum_\beta \left(\frac{4\pi e_\beta c}{B}\right)^2 n_\beta \int \frac{dk_y}{2\pi L_z}|k_y| \frac{\pi|\psi|^2(x, x, k_y, 0, -ik_y V_y)}{|\partial V_y/\partial x|}. \tag{16.190}$$

The integral over k_y is logarithmically divergent at large k_y. In this range, the Green's function is unshielded, eqn (16.119) becoming

$$\frac{\partial^2\psi}{\partial x^2} - k_y^2\psi = \delta(x - x') \tag{16.191}$$

which implies $\psi(x, x) = 1/(2|k_y|)$ at large k_y. Substituting this form into eqn (16.190) yields, to logarithmic accuracy

$$D_{\alpha\beta}^{2D} = \sum_\beta \left(\frac{4\pi e_\beta c}{B}\right)^2 \frac{n_\beta}{4L_z|S|} \ln\left(\frac{k_{y\,\max}}{k_{y\,\min}}\right) \tag{16.192}$$

where $k_{y\,\max}$ and $k_{y\,\min}$ are cutoffs determined, as always, by physics outside of the model equations used to obtain the result (Chavanis 2000; Jin and Dubin 2001; Dubin 2003). We neglect for the moment the rather subtle effects that enter into these cutoffs,

and instead compare eqn (16.192) to our previous expression for $D_{\alpha\beta}$, eqn (16.187). This expression included only $k_z \neq 0$ terms, and is now referred to as $D^{3D}_{\alpha\beta}$. The ratio of $D^{2D}_{\alpha\beta}$ to $D^{3D}_{\alpha\beta}$ is roughly

$$\frac{D^{2D}_{\alpha\beta}}{D^{3D}_{\alpha\beta}} \sim \frac{\omega_B}{S}, \tag{16.193}$$

where we have neglected constants of order unity, and the logarithmic factors.

Thus, when $\omega_B > S$, the $k_z = 0$ (2-dimensional) contribution to the diffusion dominates. Also, note that the 2D contribution scales with B as B^{-1} (since $S \propto 1/B$) rather than B^{-2}.

The effect of large axial bounce frequency on transport can be understood from the following simple argument. The rapid axial bounce motion can be averaged out, which effectively replaces the particles by rods of charge with charge per unit length $q \equiv e/L_z$. The charged rods then $\mathbf{E} \times \mathbf{B}$ drift in the electric field created by the other rods. This model is also called a point vortex gas, for reasons that will soon become apparent. The equations of motion for this 2-dimensional system of charged rods are

$$\begin{aligned} \frac{dx_i}{dt} &= -\frac{c}{B}\frac{\partial}{\partial y_i}\phi(x_i, y_i, ..., x_N, y_N); \\ \frac{dy_i}{dt} &= \frac{c}{B}\frac{\partial}{\partial x_i}\phi(x_1, y_1, ..., x_N, y_N). \end{aligned} \tag{16.194}$$

As first noted by Taylor and McNamara (1971), the magnetic field can be scaled out of these equations by scaling time as $\bar{t} = ct/B$. Thus, a change in B simply changes the time scale of the dynamics without affecting the orbits in any other way. An increase in B by a factor of 2 slows the dynamics down by this factor. Particle flux due to diffusion or viscosity must therefore scale as B^{-1}. For the case of diffusion, the generalized Fick's law [eqn (16.180)] then implies that diffusion coefficients scale as $1/B$ for this system, as we obtained in eqn (16.192). Also, for viscosity, particle flux proportional to $1/B$ implies that $\lambda \propto B^1$ [see eqn (16.170)] and recall that $V_y \propto 1/B$), which is larger than the B^0 scaling obtained previously. Viscosity and particle diffusion are increased because the correlation time of density and potential fluctuations is now set by slow $\mathbf{E} \times \mathbf{B}$ drift motion rather than relatively fast motion along the magnetic field.

Also, this 2D plasma model implies heat flux scaling as $1/B$ as well, but this flux is only a small correction to the previous $O(B^0)$ results of Lectures 3 and 5.

We can use the intuition gained from the model of the plasma as a collection of charged rods to understand eqn (16.192) in more detail. Rods with charge per unit length $q = e/L_z$ drift past one another due to the flow shear, $S = \partial V_y/\partial x$, and as they interact they take an $\mathbf{E} \times \mathbf{B}$ drift step across the magnetic field. The $\mathbf{E} \times \mathbf{B}$ drift motion of 2 rods in a shear flow S is an integrable problem in Hamiltonian mechanics (Jin and Dubin 2001), described by the Hamiltonian

$$H(x, y) = -\frac{1}{2}\frac{qB}{c}Sx^2 + q^2 \ln(2\sqrt{x^2 + y^2}) \tag{16.195}$$

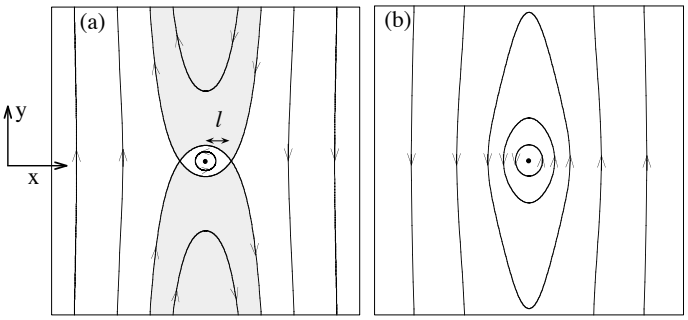

Fig. 16.12 Streamlines for rods in a shear flow. (a) $qS < 0$ (retrograde flow); (b) $qS > 0$ (prograde flow).

where $\pm(x, y)$ is the location of each rod compared to the center of charge, and the dynamics is viewed in a frame where the center of charge is stationary. The equations of motion for one of the two rods are

$$\frac{dx}{dt} = \frac{c}{qB}\frac{\partial H}{\partial y} \ , \quad \frac{dy}{dt} = -\frac{c}{qB}\frac{\partial H}{\partial x}, \tag{16.196}$$

and the other rod is at $-(x, y)$. The rods move along surfaces of constant H shown in Fig. 16.12a and 16.12b for the two cases $qS < 0$ and $qS > 0$. When $qS < 0$ (termed "retrograde flow") a separatrix exists in the flow, whose width is

$$\ell = \sqrt{-qc/BS} \tag{16.197}$$

at $y = 0$. Rods in the shaded region of the figure take an $\mathbf{E} \times \mathbf{B}$ drift step $\Delta x \sim \ell$. The number of such interactions per unit time is roughly $S\ell^2 n_{2D}$ as rods are swept past one another by the flow, where $n_{2D} \equiv nL_z$ is the number of rods per unit area. Thus, the diffusion coefficient is roughly

$$\begin{aligned} D^{2D} &\sim S\ell^2 n_{2D} \cdot \ell^2 \\ &= \left(\frac{qc}{B}\right)^2 \frac{n_{2D}}{|S|}, \end{aligned} \tag{16.198}$$

in agreement with the scaling of eqn (16.192).

In fact, collisions between rods with impact parameters $\rho \lesssim \ell$, that result in reflections as depicted in Fig. 16.12a, are not included in eqn (16.192) (which was derived through linearization, i.e. integration along unperturbed orbits). The linearization requires the orbits are only slightly perturbed, and so eqn (16.192) applies only for impact parameters larger than ℓ. This sets one estimate for $k_{y\,\max}$; $k_{y\,\max} \sim \ell^{-1}$. For impact parameters less than ℓ, a detailed Boltzmann calculation of the diffusion (Jin and Dubin 2001) yields

$$D^{2D}_{\text{Boltzmann}} = 16\left(\frac{qc}{B}\right)^2 \frac{n_{2D}}{|S|} \ln^2(0.17 n_{2D}\ell^2). \tag{16.199}$$

This result must be added to eqn (16.192) to obtain the total diffusion. Equation (16.199) is only valid if $n_{2D}\ell^2 < 1$, which requires strong shear or low density. For $n_{2D}\ell^2 \gtrsim 1$ (large densities, low shear), the two particle picture of collisions shown in Fig. 16.12a is incorrect because other particles intervene. Only eqn (16.192) is required to describe the diffusion in this high density low shear regime.

Note however, that if $qS > 0$ (termed "prograde flow"), there is no separatrix in the flow (see Fig. 16.12b); instead, two rods trap one another in their mutual interaction, circulating indefinitely. Diffusive steps are only taken when these trapped rods interact with others, disrupting the circulation. No rigorous theory for this situation has been developed, and we do not expect eqn (16.192) to accurately describe this case. Thus, eqn (16.192) only applies to the case $qS < 0$ [or for multiple species, $(q_\alpha + q_\beta)S < 0$; see Dubin (2003)].

Another issue that must be addressed is the physics of the cutoffs in the logarithmic divergence of eqn (16.192), $k_{y\,\min}$ and $k_{y\,\max}$. These wavenumbers are set, respectively, by maximum and minimum distance scales along the flow direction. The maximum distance scale is determined by the system size. In a rotating plasma with circular cross section transverse to the magnetic field, the maximum distance at radius r is the circumference $2\pi r$, which sets $k_{y\,\min} \sim 1/r$. The minimum distance scale is set by two possibilities: the distance ℓ (see Fig. 16.12a) or a distance $\delta = \sqrt{D^{2D}/|S|}$ determined by the diffusion itself. Particles separated by a distance less than δ diffuse apart before they shear apart, contradicting the assumption of integration along unperturbed orbits used in deriving eqn (16.192). Thus, we take $k_{y\,\max} = 1/\max(\delta, \ell)$.

One more issue must be addressed before we compare eqn (16.192) to results from experiments and computer simulations. Equation (16.192) indicates that as the flow shear S decreases, transport increases. This is because adjacent rods have less relative velocity and interact for a longer time as S decreases. However, as $S \to 0$ this breaks down: the relative motion of rods is no longer set by the shear flow, but rather by the diffusion process itself. Rods diffuse apart a distance of order the Debye length λ_D at a rate of order D^{2D}/λ_D^2. If we simply replace S by this rate in eqn (16.192) we obtain (assuming $\lambda_D > \ell$),

$$\begin{aligned}(D^{2D})^2 &\sim \left(\frac{4\pi ec}{B}\right)^2 \frac{n\lambda_D^2}{4L_z} \ln\left(\frac{r}{\lambda_D}\right) \\ &= \left(\frac{4\pi qc}{B}\right)^2 \frac{n_{2D}\lambda_D^2}{4} \ln\left(\frac{r}{\lambda_D}\right). \end{aligned} \tag{16.200}$$

This is an estimate of the diffusion coefficient in a shear-free plasma in the 2-dimensional limit, first put forward in Taylor-McNamara (1971) and Dawson *et al.* (1971). If the temperature is sufficiently high so that the Debye length is greater than the plasma radius r_p, one should replace λ_D by r_p, and set the logarithm to unity since its argument is only an estimate. In this case the result is usually referred to as Taylor-McNamara diffusion, and can be written as

$$D^{TM} = \frac{qc}{2B}\sqrt{\frac{N}{\pi}} \tag{16.201}$$

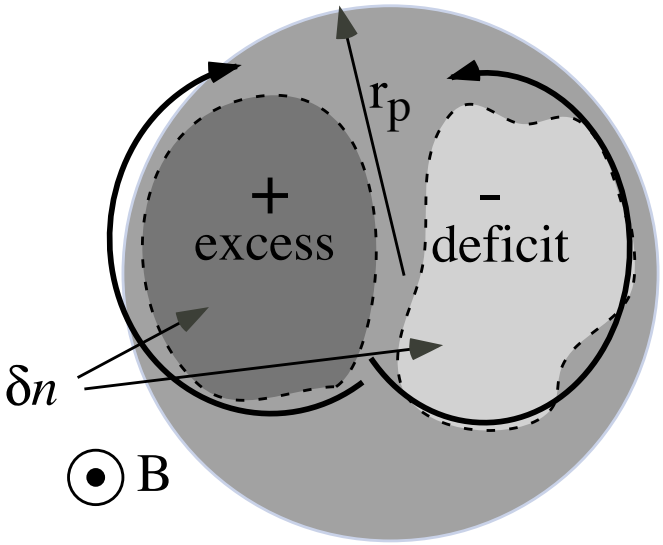

Fig. 16.13 Sketch of Dawson-Okuda vortices.

where $N = \pi r_p^2 n_{2D}$ is the number of charges in the plasma. Another way to understand diffusion in this limit is through the action of long-wavelength density/potential fluctuations (see Fig. 16.13). A density fluctuation with size scale of order r_p would, on average, have a magnitude of order $\delta n_{2D} \sim \sqrt{N}\, n_{2D}/N$ and cause an $\mathbf{E} \times \mathbf{B}$ drift velocity of order $(c/B)\, q\delta n_{2D} r_p$. The "diffusive step" is of order r_p in such a fluctuation, and the rate of the steps is the circulation rate in the fluctuation, $(c/B)\, q\delta n_{2D}$. Thus,

$$\begin{aligned} D^{TM} &\sim \frac{c}{B} q\delta n_{2D}\, r_p^2 \\ &= \frac{qc}{\pi B}\sqrt{N}, \end{aligned} \tag{16.202}$$

which has the same scaling as eqn (16.201). If we replace the spatial size r_p of these fluctuations by λ_D, we recover the scaling of eqn (16.200). These fluctuations are often referred to as "convective cells" or "Dawson-Okuda vortices." For nonzero shear, the Dawson-Okuda vortices are pulled apart by the flow shear, reducing the radial scale of the diffusive steps. This is why D^{2D} given by eqn (16.192) decreases with increasing S.

Experiments and simulations have been performed on plasmas in the 2D regime, to test eqn (16.192). In the simulations, N identical charged rods are randomly placed in a plasma with circular cross-section, and their 2D $\mathbf{E} \times \mathbf{B}$ drift motion is followed using eqn (16.194). To add flow shear, an external radial electric field is also applied, and radial diffusion of the rods is measured. The resulting diffusion coefficient is plotted versus N for four different shear rates in Fig. 16.14. In the figure $\gamma = 4\pi qc/B$ in

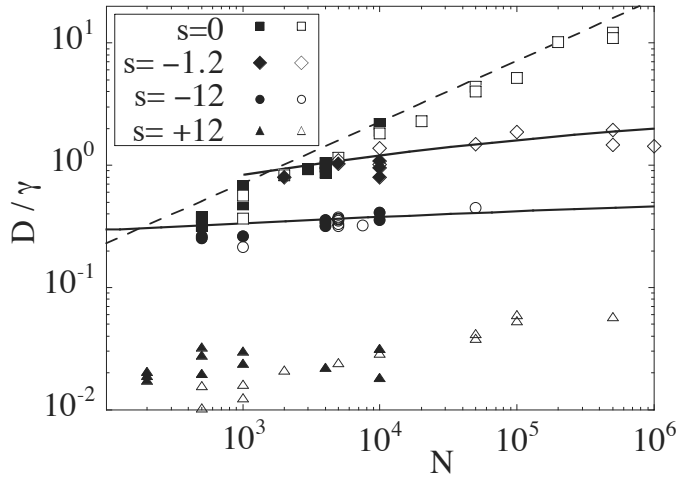

Fig. 16.14 Diffusion measured in simulations for 4 different shear rates, versus number of rods N. Here $s = SB/(2\pi qcn_{2D})$ is a scaled shear rate and $\gamma = 4\pi qc/B$. Solid lines are eqn (16.192) added to eqn (16.199). Dashed line is eqn (16.201).

the "circulation" associated with a rod (which happens to have units of a diffusion coefficient) and $s = 2S/n_{2D}\gamma$ is a scaled shear rate. For $s < 0$ eqn (16.192) (with eqn (16.199) added) accurately predicts the diffusion. For $s = 0$ eqn (16.201) works well. [Note that random placement of the rods corresponds to infinite temperature and hence $\lambda_D \gg r_p$, so eqn (16.201) should be used rather than eqn (16.200).]

For $s > 0$, corresponding to the case $qS > 0$ for which eqn (16.192) is not expected to apply, the measured diffusion is an order of magnitude less than eqn (16.192) predicts (triangles). As yet there is no theory available for this case.

Experiments on Mg^+ ion plasmas have also measured diffusion, as discussed in Lecture 2, and when $\omega_B > |S|$ the experiments do observe the expected scaling of D with shear (Fig. 16.15). When shear is large enough so that $\omega_B/|S| < 1$, the plasma is in the 3D regime described by eqn (16.59); but when shear is smaller, the results show the expected increase of the diffusion as shear decreases, although the magnitude is off by about a factor of 2 compared to eqn (16.192) (Driscoll *et al.* 2002). For comparison, the Taylor-McNamara zero-shear result of eqn (16.202) is also shown.

16.6.1 Continuum limit and 2D Euler flow

So far these lectures have focused on collisional transport theory. However it is worth mentioning that the model introduced in this lecture, of a magnetized plasma as a collection of charged rods moving via $\mathbf{E} \times \mathbf{B}$ drift dynamics in 2 dimensions, has interesting implications beyond the area of transport theory. We briefly review some aspects of the extensive research in this area. In the continuum limit of the model (i.e., neglecting collisions) the system is described by the Vlasov equation for the 2D rod density $n_{2D}(x, y, t)$,

$$\frac{\partial n_{2D}}{\partial t} - \frac{c}{B}\nabla\phi \times \hat{z} \cdot \nabla n_{2D} = 0 \tag{16.203}$$

where the electrostatic potential $\phi(x, y, t)$ is related to n_{2D} via the 2D Poisson's equation

$$\nabla_\perp^2 \phi = -4\pi q n_{2D}. \tag{16.204}$$

This plasma model is isomorphic to a two-dimensional neutral inviscid fluid, which is described by Euler's equations for the vorticity $\zeta(x, y, t) = \hat{z} \cdot \nabla \times \mathbf{V}(x, y, t)$, where $\mathbf{V}$ is the flow velocity in the x-y plane. Euler's equations are

$$\frac{\partial \zeta}{\partial t} + \mathbf{V} \cdot \nabla \zeta = 0 \tag{16.205}$$

where the fluid velocity $\mathbf{V}$ is related through the incompressibility condition $\nabla \cdot \mathbf{V} = 0$ to a stream function $\psi(x, y, t)$,

$$\mathbf{V} = \hat{z} \times \nabla \psi, \tag{16.206}$$

and ψ is given in terms of ζ by

$$\nabla_\perp^2 \psi = \zeta. \tag{16.207}$$

Comparing eqns (16.203)–(16.204) to eqns (16.205)–(16.207), we see that vorticity ζ is related to density n_{2D} through

$$\zeta = -4\pi q n_{2D} \frac{c}{B}, \tag{16.208}$$

and the stream function is related to the electrostatic potential via

$$\psi = \frac{c\phi}{B}. \tag{16.209}$$

Using these relations, a 2D plasma can be employed to study 2D Euler flow. The 2D Euler equations are a useful paradigm for various fluid flows occurring in nature, from turbulence in soap films to large-scale atmospheric flows such as hurricanes, or Jupiter's great red spot. Also, eqs (16.194), describing the $\mathbf{E} \times \mathbf{B}$ motion of charged rods, are the same as the equations of motion for a point vortex gas consisting of N point vortices with identical circulation $\gamma = 4\pi qc/B$. (Circulation is the area integral over the vorticity.) The point vortex gas has been employed as a model for turbulent flow for many years.

Experiments on pure electron plasmas, carried out in the 2D regime where $\omega_B \gg \nu, S$, have investigated several aspects of 2D Euler flow, and have observed some striking new phenomena. In these experiments, the electron plasma is trapped in a Penning trap configuration similar to those used in the previously-described transport experiments using Mg^+ ion plasmas; see Fig. 16.4. One must change the sign of the confinement voltages to contain electrons rather than ions.

To diagnose the plasma the end confinement electrode voltage is rapidly brought to ground, allowing the electrons to stream out along the magnetic field. An accelerating voltage increases their parallel energy to around 10 kV and they impact a phosphor screen (not shown in the figure). A camera image of the glowing phosphor provides

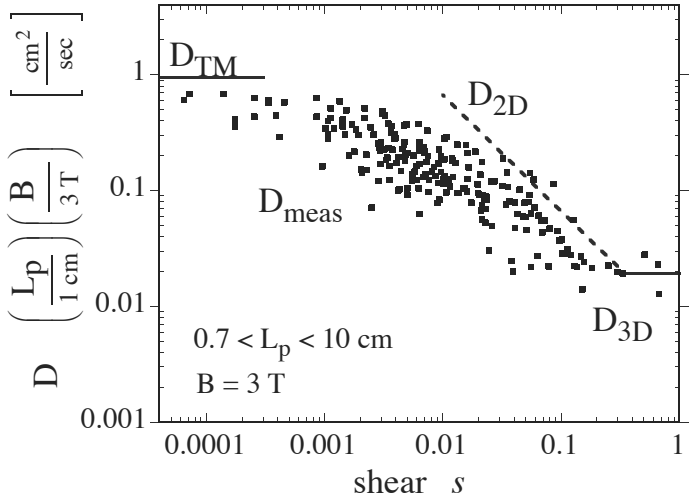

Fig. 16.15 Experimental measurement of diffusion in the 2D regime compared to eqn (16.192). Here s is the scaled shear rate (see Fig. 16.14). Here the plasma length is referred to as L_p.

a direct measurement of $n_{2D}(x, y, t)$. Although the measurement is destructive, by repeatedly creating the same initial condition and allowing it to evolve for different times, a time history for $n_{2D}(x, y, t)$ can be built up, providing a complete record of the dynamics of the 2D flow. Movies starting from various initial conditions can be found on the nonneutral plasma website, http://nnp.ucsd.edu.

Figure 16.16 shows a sequence of images in which two vorticity patches (electron columns) undergo merger (Fine *et al.* 1991). Well-separated vortices would simply rotate around one another due to their self-interaction. However, if the vortices are sufficiently closely spaced, the flow field of one distorts the other. This distortion lowers their self-energy, and in order to conserve total energy the vortices must therefore move closer together. (This energy argument is more intuitive if one thinks of the vortices as electron columns; the energy is just the repulsive potential energy of the columns, including their self and mutual interaction.) This results in merger when the vortices are sufficiently close together.

Figure 16.17 shows the merger time as a function of $2D/2R_v$ where $2D$ is the initial separation and $2R_v$ is the initial vortex diameter. The time for merger increases by a factor of 10^4 as D/R_v passes from 1.5 to 1.8. These results are in good agreement with analytical theory and numerical computation for 2D ideal fluids (Moore and Saffman 1975; Saffman and Szeto 1980; Rossow 1977; Melander *et al.* 1988). The eventual merger for $D/R_v \gtrsim 2$ is caused by slow expansion of the vortices due to the weak viscous effects analyzed previously in these lectures.

This merger process is an important element in the dynamics of more complex 2D flows. An example is shown in Fig. 16.18 (Fine *et al.* 1995). Starting from a highly-unstable filamented initial condition, the filaments of vorticity quickly form many

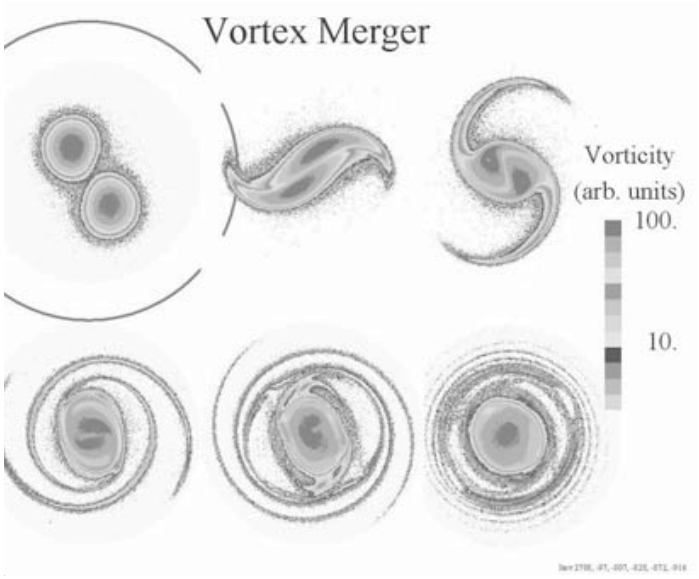

Fig. 16.16 Merger of two like-sign vortices.

intense vortices. The vortices subsequently advect chaotically, and merge when they are advected within the merger radius. The mergers are a manifestation of the "inverse cascade" (Kraichnan 1967) of energy in 2D turbulence: mergers take filamented vorticity and clump it into larger-scale vorticity patches.

The relaxation of 2D turbulent flow to an equilibrium state has been considered by many authors. Some theories describe the relaxation process as ergodic mixing of the vorticity, resulting in maximization of an entropy functional $S[\zeta]$ (Onsager 1949; Joyce and Montgomery 1973; Smith 1991; Lynden-Bell 1967; Miller *et al.* 1992; Robert and Sommeria 1992). Other theories extremize other functionals, such as the enstrophy $Z_2(\zeta) = \int d^2r\zeta^2$ (Bretherton and Hardvogel 1976; Leith 1984). Such theories predict smoothly-varying (though not necessarily monotonic) equilibrium states, unlike the rather sharply-peaked final vorticity observed in Fig. 16.18. Evidently, maximum entropy theories do not explain the final state in these experiments because the turbulent mixing is not fully ergodic–vorticity trapped in the cores of strong vortices does not ergodically mix throughout the flow.

Other theories (McWilliams 1990; Carnevale *et al.* 1991, Weiss and McWilliams 1993) describe the turbulent relaxation process as a series of merger events, resulting ultimately in one final vortex. For the flow depicted in Fig. 16.18 such theories describe the evolution rather well (Fine *et al.* 1995). However, a slightly different unstable initial condition results in a very different final state (Fig 16.19). In this evolution merger events occur initially, but then stop and the final state consists of several strong vortices in a rigidly rotating regular pattern. These patterns are referred to as vortex crystal states, and were not predicted by any previous theory of relaxing 2D inviscid turbulence.

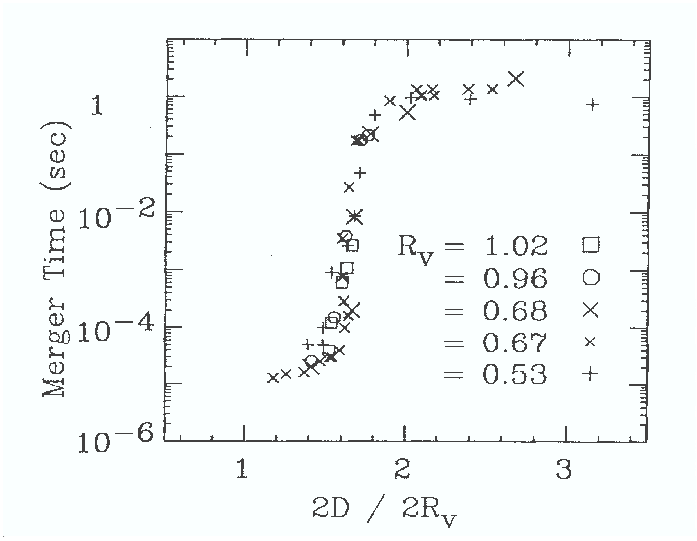

Fig. 16.17 Merger time versus vortex separation.

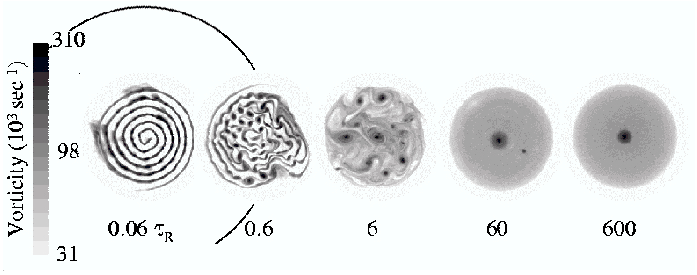

Fig. 16.18 Free relaxation of a turbulent flow.

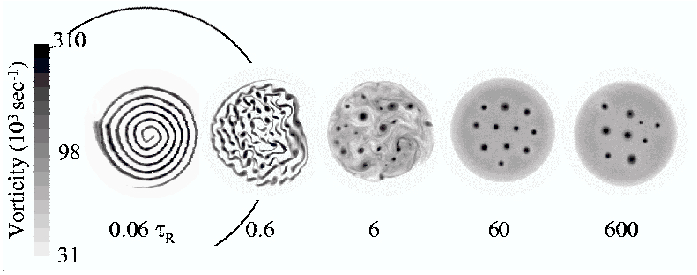

Fig. 16.19 Formation of a vortex crystal from relaxation of 2D turbulence. Here τ_R is the overall rotation time of the vorticity patch.

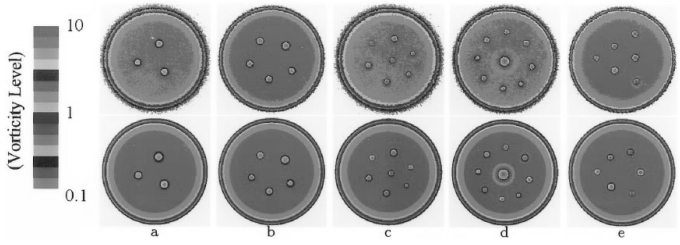

Fig. 16.20 Comparison of experimental crystal patterns (upper) to regional maximum entropy theory (lower).

It is now understood that vortex crystal states occur because the strong vortices interact with a low-vorticity background that surrounds them. This background may be present initially, or in the case of Fig. 16.19 may be produced by the merger process as filaments of vorticity are thrown off (see Fig. 16.16) and subsequently mixed. As the strong vortices mix the background, they maximize its entropy and this causes the strong vortices to "cool," falling into a minimum energy state. In fact, by maximizing the entropy $S[\zeta_b]$ of the background vorticity ζ_b, subject to the constraint that there are a given number of strong vortices, the observed vortex crystal patterns can be predicted (Fig. 16.20). This is referred to as "regional maximum entropy theory" since only the background is ergodically mixed to a maximum entropy state, while the vorticity trapped in the strong vortices is not mixed (Jin and Dubin 1998).

The number of strong vortices in the final state is determined by a competition between the merger process and the cooling process. The rate at which mergers occur slows as the number of vortices decreases, and the rate of cooling increases as the background vorticity increases. Both effects act to eventually arrest mergers and form vortex crystals. However, since both the merger and cooling process involve chaotic dynamics, we can only estimate the number of strong vortices in the final state (Jin and Dubin 2000).

The interaction of strong vortices with a lower-vorticity background is important in the formation of vortex crystals, and is also important in a number of other applications. For instance, the motion of hurricanes on a rotating planet is influenced by the north-south gradient in the Coriolis parameter, which can be thought of as a (potential) vorticity gradient (Rossby 1948; Liu and Ting 1987; Carnevale *et al.* 1991; Reznik 1992; Smith 1993; Sutyrin 1994). The location of Jupiter's great red spot, and of other storms, can also be understood as due to the interaction of the storms with the background vorticity gradients due to Jupiter's strong zonal winds (Schecter *et al.* 2000).

Figure 16.21 shows that clumps (strong vorticity excesses) ascend a background vorticity until they reach a peak, whereas holes (strong vorticity deficits) descend the gradient (Rossby 1948; Liu and Ting 1987). This gradient-driven separation helps organize storms into bands of like-sign vortices on planets (such as Jupiter) with strong zonal winds, with holes in vorticity troughs and clumps at vorticity peaks (Schecter *et al.* 2000). The opposite motion of clumps and holes can be understood by momentum

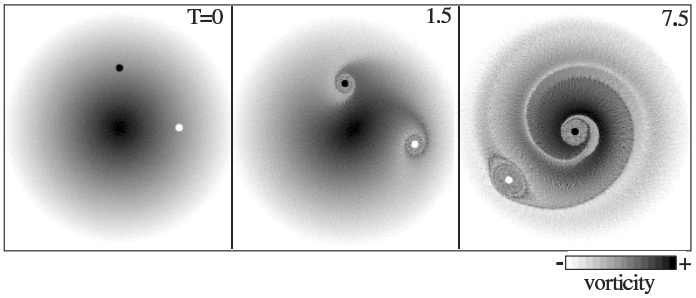

Fig. 16.21 Motion of a clump (and a hole) up (and down) a background vorticity gradient.

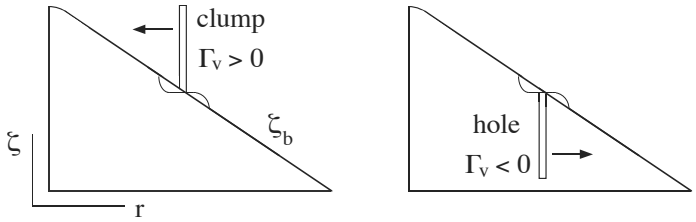

Fig. 16.22 Local mixing of the background vorticity increases $\langle r^2 \rangle_b$. By conservation of P_θ, clumps and holes react oppositely.

conservation. When there is just one strong vortex in an isolated background vorticity patch, the conserved angular momentum consists of two pieces: a background contribution and a vortex contribution:

$$P_\theta = \gamma_b \langle r^2 \rangle_b + \gamma_v r_v^2, \tag{16.210}$$

where $\gamma_b > 0$ is the circulation of the background, $\langle r^2 \rangle_b$ is the mean-square radius of the background patch, γ_v is the circulation of the strong vortex (positive for clumps and negative for holes) and r_v is the radial location of the vortex. The strong vortex mixes and flattens the θ-averaged background vorticity, as is visible in Fig. 16.21, and is shown schematically in Fig. 16.22. As the background is leveled, it is evident from Fig. 16.22 that $\langle r^2 \rangle_b$ increases. To conserve P_θ, eqn (16.210) implies that r_v^2 must decrease for clumps ($\gamma_v > 0$), and increase for holes ($\gamma_v < 0$).

The radial speed of clumps moving up a vorticity gradient can also be predicted. In fact we have already calculated it, in Lecture 5. There, the flux of a species α due to a density gradient in a *different* species β was given by

$$\Gamma_\alpha = \bar{D}_{\alpha\beta} \frac{\partial n_\beta}{\partial r} \tag{16.211}$$

(changing from planar to cylindrical coordinates). This flux is $\Gamma_\alpha = n_\alpha v_r$ where v_r is the radial velocity of species α up the density gradient due to species β. However, in the 2D regime we have seen that vorticity and density are the same, so eqn (16.211)

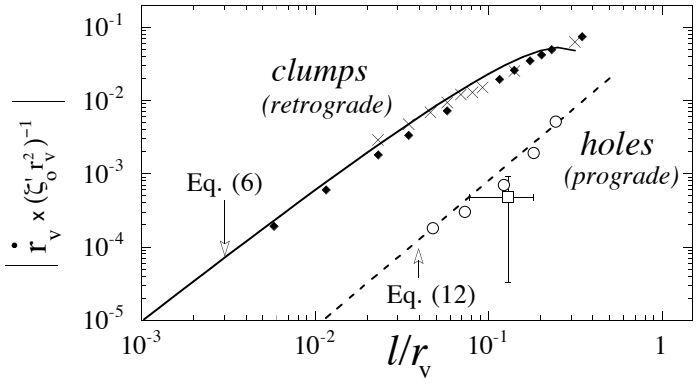

Fig. 16.23 Radial velocity of clumps and holes versus ℓ/r_v, where $\ell = \sqrt{|\gamma_v/2\pi S|}$. Here Eq. (6) and Eq. (12) refer to equations in Schecter and Dubin (1999). The solid line is eqn (16.212). The dashed line is a mix and move estimate.

predicts the velocity of a species α vortex up the vorticity gradient due to another species β. Using eqns (16.192) and (16.182) we then obtain

$$v_r = \frac{\gamma_v}{4|S|} \ln\left(\frac{r_v}{\ell}\right) \frac{\partial \zeta_b}{\partial r_v}(r_v), \tag{16.212}$$

where we have converted from plasma units to fluid units using eqn (16.208), and the circulation of the strong vortex (species α) is related to charge q_α per unit length as $\gamma_v = -4\pi c q_\alpha / B$. Equation (16.212) works well in predicting the speed of strong vortices up or down a background gradient, *provided that* $\gamma_v S < 0$, the case of retrograde flow discussed previously (see Fig. 16.12a). For retrograde flow, most of the flow is only slightly perturbed by the strong vortex, and so a quasilinear calculation using integration along unperturbed orbits is valid. However for prograde flow with $\gamma_v S > 0$ (Fig. 16.12b) the flow around the strong vortex is trapped and integration along unperturbed orbits does not work. For the background vorticity patch shown in Fig. 16.21, clumps are retrograde ($\gamma_v S < 0$) and holes are prograde ($\gamma_v S > 0$), so eqn (16.212) works for clumps but not holes. Holes are observed to move an order of magnitude slower than the clumps–see Fig. 16.23. This same nonlinear effect was responsible for the observed decrease in diffusion in simulations where $qS > 0$–see Fig. 16.14. As yet, no rigorous theory describes the velocity of prograde holes, although a "mix and move" estimate does appear to work (Schecter and Dubin 1999, Schecter *et al.* 2000).

16.6.2 Acknowledgments

The author thanks the organizers of the Les Houches lectures for the opportunity to contribute to the workshop. The author also thanks Jo Ann Christina for typing and proofreading the manuscript, Prof. C. F. Driscoll and Dr. F. Anderegg for useful scientific discussions, and Prof. T. M. O'Neil for many years of advice and encouragement.

References

Anderegg, F., Huang, X.-P., Driscoll, C. F., Hollmann, E. M., O'Neil, T. M. and Dubin, D. H. E. (1997). Test particle transport due to long range interactions. *Physical Review Letters*, **78**, 2128-31.

Braginskii, S. I. (1958). Transport phenomena in a completely ionized two-temperature plasma. *Sov. Phys. JETP*, **6**, 358–69.

Braginskii, S. I. (1965). Transport processes in a plasma. *Review of Plasma Physics, Vol. 1* (edited by M.A. Leontovitch). Consultants Bureau, New York, pp. 205–311.

Bretherton, F. P. and Haidvogel, D. B. (1976). Two- dimensional turbulence above topography. *J. Fluid Mech.*, **78**, 129–54.

Carnevale, G. F., Kloosterziel. R. C. and Van Heijst, G. J. F. (1991). Propagation of barotropic vortices over topography in a rotating tank. *J. Fluid Mech.*, **233**, 119–39 (1991).

Chavanis, P.-H. (2000). Quasilinear theory of the 2D Euler equation. *Physical Review Letters*, **84**, 5512–5.

Chen, F. (1974). *Introduction to plasma physics*. Plenum Press, New York.

Dawson, J. M., Okuda, H. and Carlile, R. N. (1971). Numerical simulation of plasma diffusion across a magnetic field in two dimensions. *Physical Review Letters*, **27**, 491–4.

Driscoll, C. F., Anderegg, F., Dubin, D. H. E., Jin, D.-Z., Kriesel, J. M., Hollmann, E.M. and O'Neil, T. M. (2002). Shear reduction of collisional transport: Experiments and theory. *Physics of Plasmas*, **9**, 1905–1914.

Dubin, D.H.E. (1997). Test particle diffusion and the failure of integration along unperturbed orbits. *Physical Review Letters*, **79**, 2678–81.

Dubin, D.H.E. (1998). Collisional transport in nonneutral plasmas. *Physics of Plasmas*, **5**, 1688–94.

Dubin, D.H.E. (2003). Collisional diffusion in a two-dimensional point vortex gas or a two-dimensional plasma. *Physics of Plasmas*, **10**, 1338–50.

Dubin, D. H. E. and Jin, D.-Z. (2000). Characteristics of two-dimensional turbulence that self-organizes into vortex crystals,Ó *Physical Review Letters*, **84**, 1443–6.

Dubin, D. H. E. and Jin, D.-Z. (2001). Collisional Diffusion in a 2-Dimensional Point Vortex Gas. *Phys. Letters A*, **284**, 112–7.

Dubin, D. H. E. and O'Neil, T. M. (1988). Two-dimensional guiding-center transport of a pure electron plasma. *Physical Review Letters*, **60**, 1286–89.

Dubin, D.H.E. and O'Neil, T. M. (1997). Cross-magnetic field heat conduction in nonneutral Plasmas. *Physical Review Letters*, **78**, 3868–71.

Dubin, D. H. E. and O'Neil, T. M. (1998). Two-dimensional bounce-averaged collisional particle transport in a single species non-neutral plasma. *Physics of Plasmas*, **5**, 1305–14.

Dubin, D. H. E. and O'Neil, T.M. (1999). Trapped nonneutral plasmas, liquids, and crystals (the thermal equilibrium states). *Reviews of Modern Physics*, **71**, 87–172.

Fine, K. S., Driscoll, C. F., Malmberg, J. H., and Mitchell, T. B. (1991). Measurements of symmetric vortex merger. *Physical Review Letters*, **67**, 588-91.

Fine, K.S., Cass, A.C., Flynn, W.G. and Driscoll, C. F. (1995). Relaxation of 2D turbulence to vortex crystals. *Physical Review Letters*, **75**, 3277–80.

Spitzer, L. and Harm, R. (1952). Transport phenomena in a completely ionized gas. *Physical Review*, **89**, 977–81.

Hollmann, E. M., Anderegg, F. and Driscoll, C. F. (2000). Measurement of cross-magnetic-field heat transport due to long-range collisions. *Physics of Plasmas*, **7**, 1767–73.

Jin, D.-Z. and Dubin, D. H. E. (1998). Regional maximum entropy theory of vortex crystal formation. *Physical Review Letters*, **80**, 4434–37.

Joyce, G. and Montgomery, D. (1973). Temperature states for the two-dimensional guiding-centre plasma. *J. Plasma Phys.*, **10**, 107–21.

Kraichnan, R. (1967). Inertial ranges in two-dimensional turbulence. *Physics of Fluids*, **10**, 1417–23.

Krall, N. and Trivelpiece, A. W. (1986). *Principles of plasma physics*, San Francisco Press, San Francisco.

Kriesel, J. M. and Driscoll, C. F. (2001). measurements of viscosity in pure-electron plasmas. *Physical Review Letters*, **87**, 135003.

Leith, C. E. (1984). Minimum enstrophy vortices. *Physics of Fluids*, **27**, 1388–95.

Lifshitz, E. M. and Pietaefski, L. P. (1981). *Physical Kinetics* (1st edn) §60. Pergamon Press, Oxford.

Liu, P. L.-F. and Ting, L. (1987). Interaction of decaying trailing vortices in spanwise shear-flow. *Comput. Fluids*, **15**, 77–92.

Longmire, C. L. and Rosenbluth, M. N. (1956). Diffusion of charged particles across a magnetic field. *Physical Review*, **103**, 507–10.

Lynden-Bell, D. (1967). Statistical mechanics of violent relaxation in stellar systems. *Mon. Not. R. Astron. Soc.*, **136**, 101–21.

McWilliams, J. C. (1990). The vortices of two-dimensional turbulence. *J. Fluid Mech.*, **219**, 361–85.

Melander, M. V., Zabusky, N. J. and McWilliams, J. C. (1988). Symmetric vortex merger in two dimensions: causes and conditions. *J. Fluid Mech.*, **195**, 303–40.

Miller, J., Weichman, P. B. and Cross, M. C. (1992). Statistical mechanics, EulerÕs equation, and JupiterÕs Red Spot. *Phys. Rev. A*, **45**, 2328–59.

Montgomery, D., Joyce, G. and Turner, L. Magnetic field dependence of plasma relaxation times. *Physics of Fluids*, **17**, 2201–04.

Montgomery, D. C. and Tidman, D. A. (1964). *Plasma kinetic theory*. McGraw Hill, New York.

Moore, D. W. and Saffman, P. G. (1975). The density of organized vortices in a turbulent mixing layer. *J. Fluid Mech.*, **69**, 465-73.

O'Neil, T. M. (1985). New theory of transport due to like-particle collisions. *Physical Review Letters*, **55**, 943–6.

Onsager, L. (1949). Statistical hydrodynamics. *Nuovo Cimento Suppl.*, **6**, 279-87.

Psimopolis, M. and Li, D. (1992). Cross field thermal transport in highly magnetized plasmas. *Proceedings Royal Society: Mathematical and Physical Sciences*, **437**, 55–65.

Reif, F. (1965). *Fundamentals of Statistical and Thermal Physics*. McGraw-Hill, New York.

Reznik, G. M. (1992). Dynamics of singular vortices on a beta-plane. J. Fluid Mech., **240**, 405–32.

Robert, R. and Sommeria, J. (1992). Relaxation towards a statistical equilibrium state in two-dimensional perfect fluid dynamics. *Phys. Rev. Lett.*, **69**, 2776–9.

Rosenbluth, M. N. and Kaufman, A. N. (1958). Plasma diffusion in a magnetic field. *Physical Review*, **109**, 1–5.

Rosenbluth, M.N. and Liu, C.S. (1976). Cross-field energy transport by plasma waves. *Physics of Fluids*, **19**, 815–18.

Rossby, C. G. (1948). On displacements and intensity changes of atmospheric vortices. *J. Marine Res.*, **7**, 175–87.

Rossow, V. J. (1977). Convective merging of vortex cores in lift generated wakes. *J. Aircraft*, **14**, 283–90.

Saffman, P. G. and Szeto, R. (1980). *Physics of Fluids*, **23**, 2339-42/

Schecter, D. A. and Dubin, D. H. E. (1999). Vortex motion driven by a background vorticity gradient. *Physical Review Letters*, **83**, 2191–4.

Schecter, D. A., Dubin, D. H. E., Cass, A. C., Driscoll, C. F., Lansky, I. M. and O'Neil, T. M. (2000). Inviscid damping of asymmetries on a two-dimensional vortex. *Physics of Fluids*, **12**, 2397–12.

Simon, A. (1955). Diffusion of like-particles across a magnetic field. *Physical Review*, **100**, 1557–9.

Smith, R. K. (1993). On the theory of tropical cyclone motion. *Tropical Cyclone Disasters*, Peking Univ. Press, Beijing, p. 264–79.

Spitzer, L. (1956). *Physics of fully ionized gases* Interscience, New York.

Sutyrin, G. G. and Flierl, G. R. (1994). Intense Vortex Motion on the Beta Plane: Development of the Beta Gyres. *J. Atmos. Sci.*, **51**, 773–90.

Taylor, J. B. and McNamara, B. (1971). Plasma diffusion in two dimensions. *Physics of Fluids*, **14**, 1492–9.

Weiss, J. B. and McWilliams, J. C. (1993). Temporal scaling behavior of decaying two-dimensional turbulence. *Phys. Fluids A*, **5**, 608–21.

Part VI

Dipolar interaction in Condensed Matter